

Aus der Fachrichtung Physiologie  
der Medizinischen Fakultät  
der Universität des Saarlandes, Homburg/Saar

**Presynaptic molecular mechanisms that control quantal  
neurotransmitter discharge**

Dissertation  
zur Erlangung des Grades eines Doktors der Naturwissenschaften  
der Medizinischen Fakultät  
der Universität des Saarlandes  
2009

vorgelegt von: **Raul Guzman Castro, M.Sc.**  
geb. am: **16.04.1978 in Cartagena/Colombia**

Homburg, 2009

## **Table of content**

<b>1 Summary</b>	<b>6</b>
<b>2 Introduction</b>	<b>10</b>
2.1 General structure of synapses	10
2.1.1 Structural organization of the active zone	11
2.1.2 Postsynaptic compartment	13
2.1.3 Glutamate receptors	14
2.1.4 Release machinery	16
2.2 Aim of the study	20
<b>3 Experimental Procedure</b>	<b>21</b>
3.1 Cell Culture	21
3.1.1 Preparation and maintenance of single-cell microisland and mass culture	21
3.1.2 Hippocampal neuron preparation	23
3.2 Synaptobrevin II/VAMP2 knockout mice	25
3.3 Genotyping	25
3.3.1 Genomic DNA purification	25
3.3.2 Polymerase chain reaction	26
3.4 Lentivirus construction	28
3.4.1 Lentiviral production and transfection	28
3.5 Electrophysiology	29
3.6 Stimulations Protocols	30
3.6.1 Action potential evoked signals	30
3.6.2 Osmotic stimulation and release probability	30
3.7 Statistical analyses	31
<b>4 Results</b>	<b>32</b>
4.1 SynaptobrevinII-mRFP fully rescues synaptic transmission in Synaptobrevin deficient neurons	32

4.2 SynaptobrevinIII-mRFP knockin neurons exhibit similar exocytotic responses when compared with wild type neurons	33
4.3 Increasing the distance between the SNARE motif and the TMD of SybII gradually reduces evoked transmitter release	34
4.4 v-SNARE linker mutants alter exocytosis timing	35
4.5 Expression of v-SNARE proteins and synaptogenesis do not change with linker mutations	37
4.6 Readily releasable pool size and release probability decrease with increasing linker length	39
4.7 SybII action underlies the speeding in mEPSC time course	40
4.8 SybII action governs the time course of cleft glutamate	47
<b>5 Discussion</b>	<b>52</b>
5.1 Linkers impair priming and stimulus secretion coupling of small synaptic vesicles	52
5.2 v-SNARE action drives rapid transmitter release from SSV	53
<b>6 Bibliography</b>	<b>57</b>
<b>7 Publications</b>	<b>70</b>
<b>8 Acknowledgements</b>	<b>71</b>
<b>9 Curriculum Vitae</b>	<b>72</b>

## Abbreviations

ATP	-	adenosine triphosphate
ACh	-	acetylcholine
AP	-	Action potential
AMPA	-	$\alpha$ -amino-3-hydroxy-5-methyl-4-isoxazolepropionic acid
BoNT	-	botulinum neurotoxin
mEPSC	-	mini excitatory postsynaptic current
Ca <sup>2+</sup>	-	Calcium
CNS	-	central nervous system
CNQX	-	6-cyano-7-nitroquinoxaline-2-3dione
CPA	-	propionic acid
ConA	-	canavanin
D-AP5	-	D-2-amino-5-phosphonopentanoic acid
DNQX	-	6,7-dinitro-quinoxaline-2-3dione
DNA	-	deoxyribonucleic acid
dNTP	-	deoxyribonucleic acid
DMSO	-	dimethylsulfoxide
DMEM	-	Dulbecco's modified eagle's medium
ESPCs	-	excitatory postsynaptic currents
EDTA	-	ethylenediaminetetraacetate
fC	-	femtoCoulomb
FCS	-	Fetal calf serum
FUDR	-	Fluoro-2'-deoxyuridin
GABA	-	gamma-aminobutyric acid
GluRs	-	glutamate receptors
$\gamma$ -DGG	-	gamma-glutamyl-glycine
GLUT4	-	glutamate transporter 4
GTP	-	guanidinetriphosphate
HEPES	-	4-(2-hydroxyethyl)-tetraacetic acid
Hz	-	hertz
HBSS	-	Hank's buffered salt solution
HCl	-	hydrochloric acid
iGluRs	-	ionotropic glutamate receptors

KA	-	kainite
K <sup>+</sup>	-	potassium
Mg <sup>2+</sup>	-	magnesium
MΩ	-	megahom
mRFP	-	monomeric red fluorescence protein
mGluRs	-	metabotropic glutamate receptors
Munc 18	-	mammalian homologue of the unc-18 gene
mV	-	milivolts
nA	-	nanoampere
Na <sup>+</sup>	-	Sodium
NBQX	-	2,3-dihydroxy-6-nitro-7-sulfamoyl-benzo ( <i>F</i> ) quinixaline
NMDA	-	N-methyl-D-aspartate
NR	-	N-methyl receptor
NFS	-	<i>N</i> -ethylmaleimide-sensitive factor
pA	-	picoampere
PDL	-	poly-D-lysine
PCR	-	polymerase chain reaction
PSD	-	postsynaptic density
PM	-	plasma membrane
PNQX	-	(1,4,7,8,9,10-hexahydro-9-methyl-6-nitropyrido [3,4- <i>f</i> ]-quinoxaline-2,3-dione
Q-SNAREs	-	glutamine soluble NSF attachment protein receptors
RP	-	release probability
RRP	-	readily releasable pool
R-SNAREs	-	arginine soluble NSF attachment protein receptors
S.D.	-	standard deviation
SNARE	-	soluble NSF attachment protein receptors
SNAP-25	-	25-kDa synaptosomal-associated protein
SybII	-	Synaptobrevin II
SV	-	synaptic vesicle
SSV	-	small synaptic vesicle
TAE-buffer	-	Tris acetate EDTA buffer
TARPs	-	trans-membrane AMPA regulatory proteins

t-SNAREs	-	target soluble NSF attachment protein receptors
TMD	-	trans-membrane domain
TTX	-	tetrodo toxin
v-SNARE	-	vesicular soluble NSF attachment protein receptors
UV	-	ultraviolet
VAMP2	-	Vesicle associated membrane protein II

## 1. Summary

Regulating the neurotransmitter concentration in the synaptic cleft following a single release event modifies the strength of synaptic transmission. Previous studies have shown that the amplitude of miniexcitatory postsynaptic currents (mEPSCs) called also as “minis” depend on the concentration of neurotransmitter in the synaptic cleft (Liu et al., 1995). However, the molecular mechanism that controls the speed of neurotransmitter discharge from small synaptic vesicles remained enigmatic. SNARE proteins that are localized in opposing membranes are believed to drive fusion by using the free energy that is released during the formation of a four-helix bundle SNARE complex (Jahn et al., 2006). Recent studies using mouse chromaffin cells have demonstrated that the molecular distance between the complex-forming SNARE domain and transmembrane domain (TMD) is crucial for priming, initiation of exocytosis and fusion pore expansion (Kesavan et al., 2007). Yet, whether this scenario holds for the exocytosis of the smallest secretory vesicle type, the small synaptic vesicle, which releases its cargo about 10 fold faster than chromaffin granules (Bruns and Jahn, 1995), has remained unclear. One might speculate that these vesicles, due to their high membrane curvature, instantaneously collapse into the plasma membrane upon the first opening of the fusion pore and membrane mechanics alone suffices to drive rapid fusion pore expansion and fast transmitter release. This consideration raises the fundamental question, whether the postsynaptic quantal signal in the central nervous system (CNS) is determined by the presynaptic release machinery. To gain insight into the mechanism and implications of the SNARE-engine in the strength of synaptic transmission at CNS synapses, we expressed SynaptobrevinII (SybII) mutant proteins carrying an extended juxtamembrane region in cultured Synaptobrevin-deficient neurons. In following this strategy, we have investigated how the increase in physical distance between the SNARE domain and the TMD impacts  $Ca^{2+}$ -triggered exocytosis and quantal signalling.

The results in this doctoral thesis show that SybII controls multiple stages in the exocytosis of synaptic vesicles. They indicate that v-SNARE action determines priming of SSVs, governs their stimulus-secretion coupling in response to single action potentials and controls the speed of neurotransmitter release from single

vesicles. Thus, this study provides mechanistic insight into the exquisite temporal regulation of synaptic transmission by showing that presynaptic SNARE force is of prime importance for strength and timing of elementary SSV signals at CNS synapses.

## Zusammenfassung

Vorausgegangene Studien konnten zeigen, dass die Transmitterfreisetzung aus einem einzelnen synaptischen Vesikel die postsynaptischen Rezeptoren nicht sättigt und somit die Variabilität quantaler Signale auch auf unterschiedliche Transmitterkonzentrationen im synaptischen Spalt zurückzuführen ist. Die zugrunde liegenden molekularen Mechanismen, die die Geschwindigkeit der Neurotransmitterfreisetzung aus synaptischen Vesikeln und somit die Stärke der synaptischen Übertragung regulieren, sind jedoch unbekannt. Biochemische Studien legen nahe, dass die membran-verbindenden Interaktionen der SNARE-Proteine die zur Membranfusion benötigte Energie liefern. Aktuelle Studien in Chromaffinzellen der Maus konnten zeigen, dass eine kurze intramolekulare Distanz zwischen dem Transmembrananker und der komplexbildenden SNARE-Domäne des vesikulären Synaptobrevin II die Exozytosekompetenz („Priming“), Stimulus-Sekretionskopplung und die Expansion der Fusionspore entscheidend beeinflusst (Kesavan et al., 2007). Unklar ist jedoch, ob sich dieses Szenario auch auf die Transmitterfreisetzung aus kleinen synaptischen Vesikeln anwenden lässt. In der Tat setzen kleine synaptische Vesikel ihren Inhalt im Vergleich zu chromaffinen Granulen mit einer zehnfach schnelleren Rate frei (Bruns und Jahn, 1995). Dabei ist es denkbar, dass dieser Vesikeltyp, bedingt durch seine hohe Membrankrümmung, im Augenblick der ersten Fusionsporenöffnung unmittelbar mit der Plasmamembran verschmilzt und somit die Membranspannung die entscheidende Kraft für eine schnelle Fusionsporenexpansion und Transmitterentladung ist. Diese Überlegungen werfen die grundsätzliche Frage auf, ob sich die Eigenschaften einzelner postsynaptischer Signale im Zentralnervensystem (ZNS) durch den präsynaptischen Freisetzungsapparat beeinflussen bzw. aktiv steuern lassen. Um einen Einblick in die zugrundeliegenden Mechanismen dieser Elementarprozesse zu erlangen, haben wir untersucht, inwieweit die Aktion der SNARE-Proteine die Stärke quantaler Signale reguliert. Ausgangspunkt unserer Untersuchungen war die Überlegung, dass eine Kraftübertragung zwischen komplex-bildender SNARE-Domäne und Transmembrananker durch Verlängerung der intermittierenden Struktur beeinflussbar sein sollte. Zu diesem Zweck haben wir Insertionen unterschiedlicher Länge in die juxtamembranäre Region des Synaptobrevin II eingeführt. Ausgehend von einer SybII-defizienten Mauslinie, die nahezu keine SSV-Exozytose aufweist (Borisovska

et al., 2005), konnten wir im Rahmen einer 'Gain-of-Function' Analyse die Funktionsweise dieser mutierten Genprodukte in der Neurotransmitterfreisetzung untersuchen. Die Ergebnisse der hier vorgelegten Arbeit zeigen, dass eine kurze intramolekulare Distanz zwischen komplex-bildender SNARE-Domäne und Transmembrananker des SybII-Proteins die Exozytose synaptischer Vesikel auf mehreren Ebenen kontrolliert. So wird durch Verlängerung der juxtamembranären Domäne die Exozytosebereitschaft der synaptischen Vesikel verringert und ihre synaptische Latenz bei Stimulation einzelner Aktionspotentiale verlängert. Darüber hinaus verringern diese Mutationen die Amplitude und verlangsamen den Zeitverlauf quantaler postsynaptischer Signale. Diese Befunde weisen darauf hin, dass die Wirkung der SNARE-Proteine, durch Beeinflussung der Rate der Transmitterentladung aus einzelnen synaptischen Vesikeln, das Transmitterkonzentrationsprofil im synaptischen Spalt steuert.

Zusammengefasst legen die Befunde nahe, dass die molekulare Kraft der SNARE-Proteine das synaptische Vesikel, von seiner ersten Bereitstellung für die Exozytose bis zur eigentlichen Membranfusion, durch die unterschiedlichen Phasen der Exozytose treibt.

## **2. Introduction**

Individual nerve cells are the building blocks of the central nervous system. Although the human brain contains an extraordinary number of these cells (on the order of  $10^{11}$  neurons), which can be classified into at least a thousand different types, all nerve cells share the same basic architecture. A typical neuron has three morphologically defined regions: the cell body (soma), the metabolic center of the cell, usually gives rise to two kind of processes, several short dendrites and one long, tubular axon. Dendrites are the main apparatus for receiving incoming signals from other nerve cells, whereas the axon is the main conducting unit for carrying signals to another neurons. Near its end, the tubular axon divides into fine branches, which represents communication sites with other neurons. These communication sites are known as synapses. The high fidelity and speed of this communication process through the synapses, from a presynaptic neuron to a postsynaptic cell, are mainly depended on neurotransmitter release to transform electrical signals to chemical signals.

Other communication processes, such as the modulation of the neuronal state in entire brain regions by neuromodulators, provide an essential component of this information processing capacity. A large number of diverse neurotransmitters are used by neurons, ranging from classical fast transmitters such as glycine and glutamate over neuropeptides to lipophilic compounds and gases such as endocannabinoids and nitric oxide. Most of these transmitters are released by exocytosis.

### **2.1 General structure of synapses**

The term synapse can be used either in a structural sense or to describe an entire connection. According with the structural definition, a synapse consists of a single presynaptic active zone and postsynaptic density, together with the specialized membranes and cleft in-between. (Lisman et al., 2007). Here the electrical activity is converted into a chemical signal in the form of neurotransmitter release from the presynaptic side. After diffusing across the synaptic cleft, binding of the neurotransmitter activates ionotropic postsynaptic receptors and induces a membrane potential change in the postsynaptic neuron. (Rosenmund et al., 2003). The receptors thus determine the nature of the physiological signal. Classical

neurotransmitters such as  $\gamma$ -aminobutyric acid (GABA), glutamate, and acetylcholine (ACh) activate mostly ion channels hence mediate fast synaptic transmission, in contrast neuromodulators such as monoamines and peptides predominantly activate G-protein-coupled receptors, which activate second messengers and act on a much longer time scale (Fon, 2001).

### **2.1.1 Structural organization of the active zone**

The presynaptic active zone is defined morphologically as the site at which synaptic vesicles cluster, dock, and fuse, and physiologically as the site of neurotransmitter release (Schoch et al., 2006). The active zone is composed of an electron-dense, biochemically insoluble material located at the presynaptic plasma membrane precisely opposite the synaptic cleft. At these electron-dense region synaptic vesicles exocytosis takes place in a temporally and spatially highly coordinated manner. Typically, only small subpopulations of the 100-200 synaptic vesicles within a synapse are docked to the plasma membrane at the active zone (Figure 1). Docked vesicles have to mature into a fusion-competent primed state before their fusion with the plasma membrane can be triggered by the elevation of intracellular  $\text{Ca}^{2+}$  concentration (Rosenmund et al., 2003).

When an action potential invades a nerve terminal, voltage-gated  $\text{Ca}^{2+}$  channels open and the resulting pulse of intracellular  $\text{Ca}^{2+}$  triggers exocytosis that initiates with fusion pore opening of release-ready vesicles. In most synapses, release is stimulated by  $\text{Ca}^{2+}$  influx through P/Q- ( $\text{CaV}2.1$ ) or N-type  $\text{Ca}^{2+}$  channels ( $\text{CaV}2.2$ ), whereas the related R- ( $\text{CaV}2.3$ ) or the more distant L-type  $\text{Ca}^{2+}$  channels ( $\text{CaV}1$  series) are only rarely involved (Dietrich et al., 2003). Even at rest, synapses have a finite but low probability of release, causing spontaneous events of exocytosis that are reflected in electrophysiological recordings as miniature postsynaptic currents (Katz, 1969). Action potential evoked release triggers at least two components of release that are probably mechanistically distinct: A fast, synchronous phasic component is induced rapidly, in as little as 50  $\mu\text{s}$  after a  $\text{Ca}^{2+}$  transient develops (Sabatini and Regehr, 1996), and a slower asynchronous component continues for >1s after the action potential (Barrett and Stevens, 1972; Geppert et al., 1994; Goda and Stevens, 1994; Atluri and Regehr, 1998). Both components of release are strictly

Ca<sup>2+</sup>-dependent but change differentially upon repetitive stimulation (Hagler and Goda, 2001).

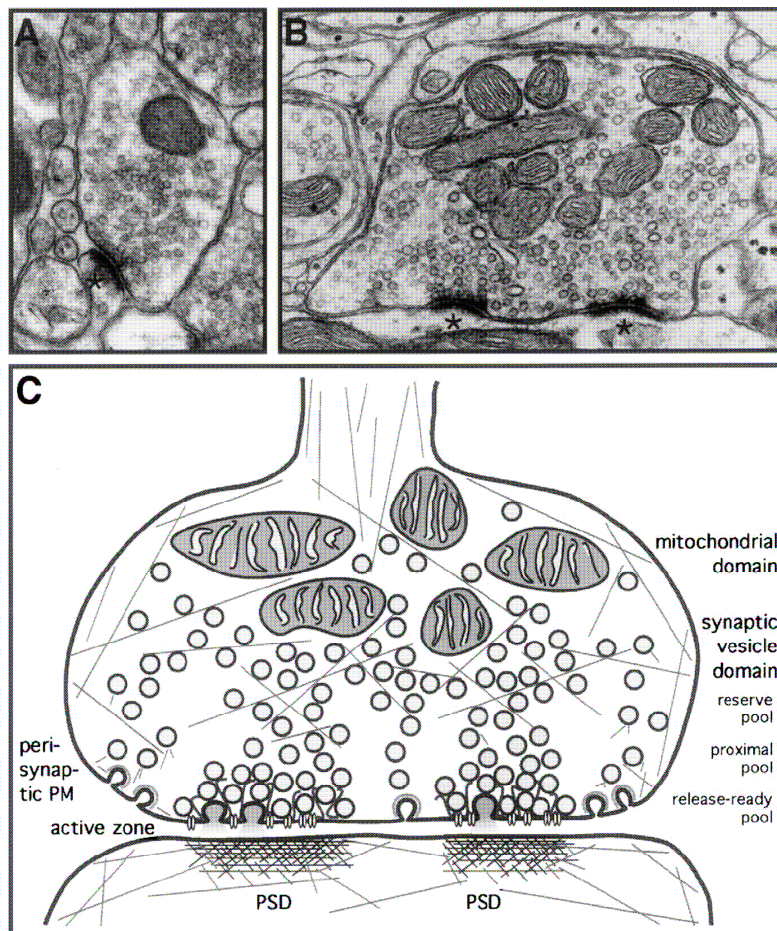


**Figure 1. Ultrastructural organization of presynaptic nerve terminals.** (A) Electron photomicrographs of the nerve terminal of an excitatory synapse in the hippocampus. (B) Other example of a vertebrate CNS synaptic terminal with two active zones and a prominent mitochondrial domain. Postsynaptic dense (PSD) projections opposite to the active zone in A and B are indicated by asterisks. (C) Schematic illustration of the structural organization of a presynaptic nerve terminal. PM, plasma membrane. (Dresbach et al., 2001).

*Mini excitatory postsynaptic currents mEPSCs.* This electrical activity-independent release is called “spontaneous”. Spontaneous neurotransmitter release is observed in the presence of tetrodotoxin (TTX), a highly specific blocker of voltage-gated Na<sup>+</sup> channels. mEPSC occur at a low frequency which indicates the low probability of release in the absence of presynaptic depolarization. Synaptic vesicles exocytosed spontaneously release neurotransmitter in packets called quantal. Each quantum is thought to represent a single synaptic vesicle (SV) and its neurotransmitter content gives rise to a postsynaptic current of small amplitude also named “minis” (Bouron, 2001). The kinetics of neurotransmitter release, diffusion and uptake by the

transporters, as well as the synaptic geometry, are all expected to influence the spatiotemporal concentration profile in the synaptic cleft, which together with the receptor properties (kinetics, density, and spatial distribution) determine the amplitude and the time course of the basic element of synaptic transmission, the mEPSC. Three hypotheses have been traditionally put forward to explain the rate of decay of the synaptic current (Jonas and Spruston, 1994). The first follows the line of argument used to explain the time course of postsynaptic current at the neuromuscular junction (Magleby and Stevens, 1972). The decay of glutamate concentration in the synaptic cleft is assumed to be very rapid, the decay time of the postsynaptic current being therefore determined by channel closure, similar to deactivation (Hestrin, 1990; Tang et. al., 1991). The second hypothesis argues that the decay of glutamate concentration is slow and that the postsynaptic current is terminated by desensitization of AMPA receptor channels (Trussell et. al., 1988; Trussell and Fischbach, 1989; Hestrin, 1992; Trussell et al., 1993; Livsey et. al., 1993). This is plausible since AMPA receptor channels desensitize very rapidly (they are the fastest desensitizing ligand-gated ion channels). According to the third hypothesis, the postsynaptic current is determined in a complex manner by the time course of deactivation and desensitization, as well as glutamate concentration (its decay has been argued between the two extremes postulated in the first and second hypothesis (Clements et. al., 1992; Barbour et. al., 1994; Tong and Jahr, 1994).

### **2.1.2 Postsynaptic compartment**

The postsynaptic compartment is represented by a patch of plasma membrane containing a highly sophisticated neurotransmitter reception apparatus and an underlying dense matrix, the postsynaptic density (PSD) (figure 1), which is located exactly opposite the transmitter release site. The neurotransmitter receptors are clustered here, anchored to the submembraneous cytoskeleton and physically linked to components of intracellular signaling pathways. At excitatory synapses, the PSD is thought to represent this complex reception apparatus, comprising various types of glutamate receptors (GluRs) that are co-clustered at these synapses. These include metabotropic GluRs (mGluRs), which mediate transmembrane signal transduction via trimeric G proteins, and ionotropic GluRs (iGluRs), which harbor an intrinsic neurotransmitter-gated cation channel. (Hollmann and Heinemann, 1994; Nakanishi and Masu, 1994).

### 2.1.3 Glutamate receptors

Glutamate is a major neurotransmitter that mediates synaptic excitation at a vast majority of synapses in the central nervous system. Glutamate is involved in many important brain functions, such as differentiation, neuronal cell survival and death, proliferation and the development of neuronal and glial cells, and plastic changes in efficacy of synaptic transmission in adult and developing brains. Previous electrophysiological and pharmacological studies have classified glutamate receptors into two distinct groups termed ionotropic receptors and metabotropic receptors (mGluRs). Glutamatergic ionotropic receptors comprise ion channels that selectively permeate cations and are subdivided into three distinct subgroups according to their selective agonists: N-methyl-D-aspartate (NMDA), kainate, and amino-3-hydroxy-5-methyl-4-isoxazolepropionate (AMPA). The last two are sometimes referred to as non-NMDA receptors; mGluRs are coupled to intracellular second messengers via G proteins and belong to a category completely different from the ionotropic receptors (Nakanishi and Masu, 1994).

AMPA receptors mediate most of the fast excitatory synaptic transmission in the CNS of vertebrates. This subfamily of the ionotropic glutamate receptors (iGluRs) consists of four subunits, GluR1–GluR4 (Hollmann and Heinemann, 1994), forming functional homo- and heterotetrameric receptor complexes (Rosenmund et al., 1998). In contrast to *N*-methyl-D-aspartate (NMDA) receptors, AMPA receptors are not permanently anchored at the synapse. Instead, they cycle rapidly in and out of the postsynaptic membrane (Malinow and Malenka, 2002). These dynamic changes in the number of synaptic AMPA receptors determine synaptic strength (Malenka and Nicoll, 1999; Liu and Cull-Candy, 2000; Lüscher et al., 2000; Man et al., 2000; Malinow and Malenka, 2002). The interactions of the cytoplasmic tails of AMPA receptors with intracellular scaffolding proteins of the postsynaptic density (PSD) are important factors in the synaptic organization of these receptors (Malinow and Malenka, 2002). The transmembrane protein stargazin (Hashimoto et al., 1999; Chen et al., 2000), defines a family of proteins termed transmembrane AMPA receptor regulatory proteins (TARPs) and was shown to support receptor trafficking and stabilization of AMPA receptors in the PSD by its interaction with PDZ (postsynaptic density-95, discs large, zonula occludens) proteins (Hashimoto et al., 1999; Chen et al., 2000). Subunits of the GluR5 through GluR7 have been found to coassemble

with KA receptors subunit KA1 or KA2 to form the KA receptor. KA receptors have relatively low affinity to glutamate but only two pharmacological drugs, concanavalin A (ConA) and cyclothiazide, can distinguish KA receptors from AMPA receptors. These non-NMDA receptors gate cation ions with relatively low conductance ( $\ll 20$  pS), are permeable to both  $\text{Na}^+$  and  $\text{K}^+$  but usually not permeable to  $\text{Ca}^{2+}$ .

*AMPA receptor agonist.* A large number of AMPA receptor agonists have been described and many of them, like AMPA itself, have been derived from classic structure activity studies using ibotenic acid, quisqualic acid and willardiine. One of the interesting aspects of AMPA receptor agonist is that they can vary dramatically in the amount of receptor desensitization that they induce. Thus, glutamate and AMPA act as a full agonist and induce rapidly desensitizing response, whereas, kainate and propionic acid (ACPA) acts as partial agonists and induce little desensitization.

*AMPA receptor antagonist.* The first somewhat selective and useful AMPA receptor antagonists were DNQX (6,7-dinitro-quinoxaline-2,3-dione) and CNQX (6-cyano-7-nitroquinoxaline-2,3-dione), these compound are high-affinity antagonist, therefore, are characterize for display slow dissociation kinetic. However, this compound also had activity at the glycine binding side on NMDA receptors. Nevertheless, they served as the starting point for various more selective competitive AMPA receptor antagonists, such as NBQX (2,3-dihydroxy-6-nitro-7-sulfamoyl-benzo (*F*) quinixaline), PNQX (1,4,7,8,9,10-hexahydro-9-methyl-6-nitropyrido [3,4-*f*]-quinoxaline-2,3-dione) (Kew et. al., 2005).  $\gamma$ -DGG ( $\gamma$ -glutamyl-glycine) is a rapidly dissociating competitive antagonist, (low affinity) which competes with glutamate during the rising phase of AMPAR-EPSCs, generates a block that is inversely related to the transmitter concentration and have been successfully used to demonstrated changes in the spatiotemporal profile of clef glutamate experienced by the AMPAR (Diamond et. al., 1997, Liu et. al., 1999; Yamashita et. al., 2003; Cathala et. al., 2005).

NMDA receptors consist of five different subunits. NR1 forms a functional homomeric receptor channel in *X. laevis* oocytes and shows all the properties characteristic of the NMDA receptors. This single NR1 polypeptide exhibits a voltage dependent  $\text{Mg}^{2+}$  block, high  $\text{Ca}^{2+}$  permeability, potentiation by a low concentration of glycine, specific responses to various NMDA receptor agonists and antagonists, inhibition by  $\text{Zn}^{2+}$ ,

and activation by polyamines. In contrast to NR1, none of the four other subunits termed NR2A-NR2D showed any receptor-channel activity in a homomeric configuration or any heteromeric expression within the members of the NR2 subunits. However, the combined expression of individual NR2 subunits with NR1 markedly potentiates current responses to NMDA or glutamate (Nakanishi and Masu, 1994). Thus, the activation of NMDA channels requires glutamate, glycine and depolarization of the cells. The receptor control cation channels of high conductance (50 pS), is permeable to  $\text{Ca}^{2+}$  as well as  $\text{Na}^{+}$  and  $\text{K}^{+}$ . D-2-amino-5-phosphonopentanoic acid (D-AP5) is the competitive antagonist of the NMDA receptors, and MK-801 can selectively block activated NMDA receptors.

#### **2.1.4 Release machinery**

Membrane fusion, in which two distinct lipid bilayer membranes are merged into one, is the common final step in the transport of proteins among intracellular compartments, the controlled release of hormones and neurotransmitters by exocytosis. Recent progress has revealed that several protein families involved in fusion are conserved from yeast to human, and are shared not only by constitutive and regulated exocytosis but also by various intracellular membrane fusion events (Rothman, 1994; Wickner and Haas, 2000). The conserved protein families include soluble *N*-ethylmaleimide-sensitive factor attachment protein receptors (SNAREs), ATPase *N*-ethylmaleimide-sensitive factor (NSF), Munc18/Sec1, Rab GTPases, and protein components of the exocyst complex. This conservation suggests that virtually all membrane fusion processes, including synaptic vesicle exocytosis, use the same common molecular machinery for fusion.

The central players in all membrane fusion events seem to be SNAREs, a superfamily of membrane-associated proteins characterized by a ~60 amino-acid  $\alpha$ -helical coiled-coil domain called the SNARE motif (Rothman, 1994; Jahn and Sudhof, 1999; Weimbs, 1997; Rizo and Sudhof, 2002). These proteins were initially categorized as v-SNAREs and t-SNAREs based upon their localization on vesicle or target membrane (Rothman, 1994), and later reclassified as R-SNAREs and Q-SNAREs according to the conserved arginine or glutamine residue in the center of their SNARE motifs (Fasshauer, 1998).

The presynaptic membrane of a neuronal axon is the site of rapid exocytic events upon cell stimulation by an action potential. In response to  $\text{Ca}^{2+}$  influx, synaptic vesicles containing neurotransmitter fuse with the presynaptic membrane and release their contents into the synaptic cleft, where they diffuse to the postsynaptic cell (Lin and Scheller, 2000). Three SNARE proteins are involved in this process: vesicle-associated membrane protein (VAMP2), (also called synaptobrevin), syntaxin 1, and the 25-kDa synaptosomal-associated protein (SNAP-25).

*VAMP2*. Vesicle associated membrane protein II (VAMP2), also known as SynaptobrevinII, was initially characterized in synaptic vesicles (Baumert et al., 1990; Trimble et al., 1988) and represents a conserved protein family from yeast to mammals (Protopopov et al., 1993; Südhof et al., 1989). Synaptobrevin is proteolyzed by clostridial neurotoxins (i.e. botulinum neurotoxin and tetanus toxin) at the presynaptic membrane and inhibit synaptic transmission (Montecucco et al., 1993). Synaptobrevin/VAMP family members are small type II membrane proteins of about 120 amino acids. Structurally, they consist of a variable region of 25–35 amino acids located at the amino terminus, followed by either one extended or two short amphipathic  $\alpha$ -helical segments predicted to form coiled-coil structures, and have a transmembrane domain located at their carboxyl terminus. The putative  $\alpha$ -helical regions, originally designated as Helix 1 (or H1) and Helix 2 (or H2) (Grote et al., 1995; Regazzi et al., 1996; Gerst, 1997), are required for these SNAREs to mediate their protein-protein interactions, as shown by studies employing in vitro binding experiments (Grote et al., 1995; Regazzi et al., 1996; Hayashi et al., 1994; Hao et al., 1997) as well as in vivo exocytosis assays, using both yeast (Gerst, 1997) and mammalian cells (Grote et al., 1995; Regazzi et al., 1996). Both helices participate in binding to the Syntaxin and SNAP-25 (Chapman and Jahn, 1994).

The use of neurotoxins and specific antibodies has shown that toxin-sensitive isoforms, like VAMP2, are involved in stimulus-coupled secretion in a variety of cell types, including neurotransmitter release from neurons (Trimble et al., 1988; Baumert et al., 1989) insulin release from pancreatic  $\beta$ -cells (Regazzi et al., 1995); zymogen granule release from pancreatic acinar cells (Gaisano et al., 1994); catecholamine release from adrenal chromaffin cells (Misonou et al., 1997); and insulin-stimulated GLUT4 translocation in adipocytes (Olson et al., 1997).

*Syntaxin 1* is a neuronal plasma membrane Q-SNARE first described as an antigen for a monoclonal antibody called HPC-1 (Inoue et al., 1992), and subsequently identified as a binding partner for synaptotagmin and the N-type calcium channel (Bennett et al., 1992; Yoshida et al., 1992). *SNAP-25* is another Q-SNARE initially identified as a brain-specific protein localized to neuronal plasma membrane via palmitoyl groups covalently attached to the cysteine residues (Oyler et al., 1989). VAMP2 and syntaxin 1 each contain a single SNARE motif adjacent to the carboxy-terminal transmembrane domain, whereas SNAP-25 contains two SNARE motifs connected by a linker region bearing the palmitoylated cysteine residues (Weimbs et al., 1997). All SNARE proteins have a cytoplasmic orientation. The four SNARE motifs from these three proteins assemble into a parallel four-stranded helical bundle to form an extremely stable ternary complex called the SNARE complex (Figure 2), (Sollner et al., 1993; Sutton et al., 1998).

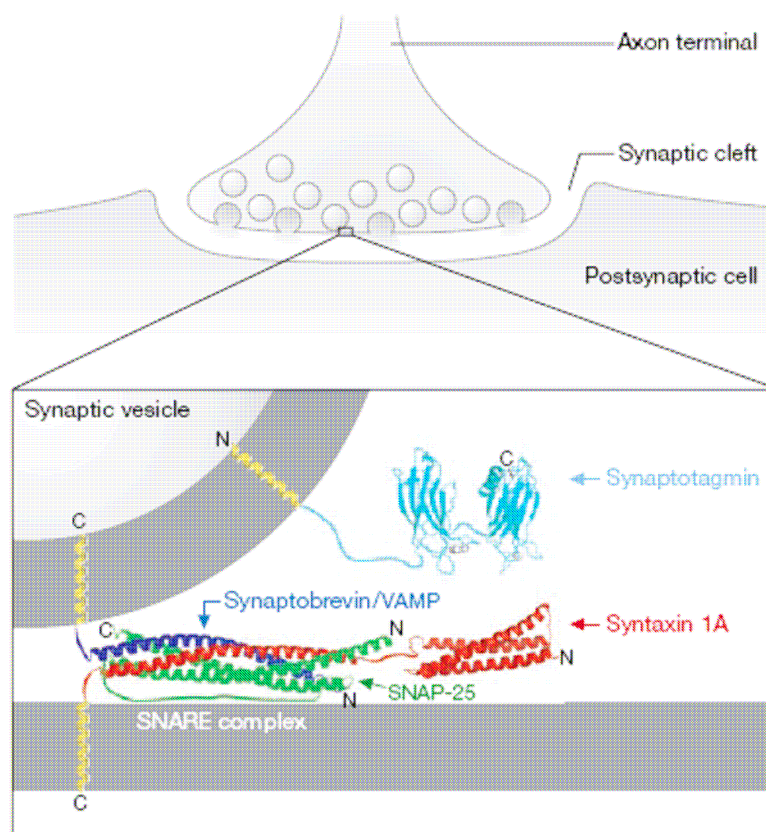


**Figure 2. Model of the neuronal SNAREs assembled into the core complex** (Carr and Munson, 2007)

Interference with the integrity of such a superhelical structure by various mutations in neuronal SNAREs inhibits synaptic vesicle exocytosis (Littleton et al., 1998; Finley et al., 2002). Moreover, specific cleavage of neuronal SNAREs by clostridial neurotoxins prevents the assembly of a stable SNARE complex and blocks neurotransmitter release without affecting the docking of synaptic vesicles (Schiavo et al., 1992; O'Connor et al., 1997). Targeted gene disruption of neuronal SNAREs in *Drosophila*, *Caenorhabditis elegans*, and mice abolishes action potential-evoked neurotransmitter release, further demonstrating an essential role for these proteins in Ca<sup>2+</sup>-stimulated synaptic vesicle exocytosis (Broadie et al., 1995; Schoch et al. 2001). Despite overwhelming evidence indicating the critical importance of neuronal SNAREs and the SNARE complex in synaptic vesicle exocytosis, their precise role in the fusion process remains controversial (Mayer, 2001; Bruns and Jahn, 2002).

## 2.2 Aim of the study

The aim of this study was to provide new insight into the presynaptic molecular mechanism that controls the speed of neurotransmitter discharge from small synaptic vesicles (SSVs). For this, we investigated how the increase in physical distance between complex-forming SNARE domain and transmembrane domain (TMD) of SynaptobrevinII (SybII) impacts  $\text{Ca}^{2+}$ -triggered exocytosis and quantal signalling. To address this issue, we expressed SybII mutant proteins carrying an extended juxtamembrane region in hippocampal neurons that are genetically deficient of SybII and nearly devoid of secretion (Schoch et al., 2001). In a gain-of-function approach individual SybII mutant proteins were examined for their ability to rescue the exocytotic responses in SybII deficient neurons. Autaptic and mass hippocampal cultures were used and fundamental synaptic parameters like, excitatory postsynaptic currents (EPSCs), mini excitatory postsynaptic currents (mEPSCs), readily releasable pool (RRP) and release probability (RP) were systematically analysed.

### **3. Experimental Procedure**

#### **3.1 Cell Culture**

##### **3.1.1 Preparation and maintenance of single-cell microisland and mass culture**

The micro-island culture technique, developed in 1976, was used to investigate the influence of non-neuronal cells and target cell innervation have upon the plasticity of rat sympathetic principal neurons with respect to the expression of adrenergic or cholinergic phenotype. Subsequent to this, microisland cultures have widely been used as a model system to study various molecular and cellular mechanisms of synaptic transmission and synaptic plasticity including the influence of synaptic proteins and trophic factors on synapse formation and neurotransmitter release (Timothy, 2006). In fact, it has been well established that this autaptic neurons are functionally indistinguishable from those *in vivo* including kinetics and pharmacological properties (Bekkers and Stevens, 1991). The basic idea of this technique is extremely simple, the aim is isolate an individual cell by restricting cell attachment and growth to small predetermined region formed by astrocytes. A particularly important characteristic is that such constraint greatly increase the probability of them forming self-innervation autaptic contacts and also increases the overall density of innervation of individual cells within the microisland. From an electrophysiological perspective, this offers several distinct advantages. First, the increased numbers of synaptic contacts greatly increase the size of evoked synaptic events, thereby facilitating their detection. Second, in single-cell cultures, all of synaptic contacts are autaptic. This greatly facilitates analysis of different release modes, since all responses induced by action potential or hypertonic solution arise from the same neuron and can be assumed to be monosynaptic, which simplifies quantal analysis of the transmitter release processes. Furthermore, only one electrode is required to both evoke and record the synaptic events (Timothy, 2006; Bekkers and Stevens, 1991).

Microisland cultures of hippocampal neurons were prepared in several steps: First, the basic principle of making microisland culture is to prepare islands of a substrate adhesive for neurons (glia cells) on a background of a nonadhesive substrate (agarose). The sterilized glass coverslip (25 mm in diameter, 1001/25, 25 mm No1,

Glaswarenfabrik Karl Hecht KG.) was covered with a thin layer of 0.15% solution of agarose (Type II-A, A-9918 Sigma.), this solution was prepared by mixing the agarose powder with sterile water and heated until the solution is just boiling, and was swirled to homogeneity. Using a 1 ml pipette a drop of agarose was applied on each coverslip. The drop of agarose should be big enough to cover the central part of the coverslip, as the drops of agarose cooled, was removed as much excess liquid agarose as possible, proportional with achieving the thinnest possible coating without contraction of the drop and the coverslips were dried at 53°C for 90 min. Coating material; 0.6 mg/ml of collagen (BD 354236) and 0.4 mg/ml of poly-D-lysine (Sigma P 6407) was sprayed using a sterile atomizer sprayer (before attempting to spray the agarose coated coverslips, few test sprays were made as to prime the atomizer and also to determine the optimum distance (usually 15 cm above and 25 cm lateral to the coverslips) and the amount of pressure to apply to the bulb in order to get a uniform coating of the desired size of the droplets/islands (20-200 µm diameter)). Once optimum conditions were determined, the agarose-coated coverslips were sprayed, left to dry for at least 1 h and sterilized under UV for 10 min before plating the astrocytes.

Astrocytes were prepared using brain cortex and hippocampal tissue, dissected from newborn of 1-2 days old mice, placed into HBSS medium (Invitrogen 24020-091) and cut it in small pieces, the tissue was gently passaged through a cell strainer with 20 ml of ice-cold DMEM (Invitrogen 31966-021). The homogenated cells were centrifuged at room temperature for 7 minutes at 1700 rpm. The cells were gently triturated using a blue tip so as to obtain a single cell suspension, seeded and grown on 75-cm<sup>2</sup> flask with 10% FCS-DMEM (10% FCS, invitrogen 10270-106, DMEM, 100 unit/ml of penicillin and 100 unit/ml of streptomycin (Invitrogen 15140-122, MITO BD Biosciences 355006) and maintained in a humidified incubator at 37°C with carbon dioxide content of 9%, Medium was replaced on next day and on each third day. Once confluent, the astrocytes were collected with Trypsin-EDTA (Invitrogen 15400-054, it was diluted 10 times with DPBS Invitrogen 14190-094), suspended and then centrifuged at 1300 rpm for 3 min. Approximately 100.000 astrocytes/ml were plated in each well of 6-well tissue culture plates on the previously coated coverslips with 10% FCS-DMEM. After astrocytes were confluent on the micro-island, neurons were plated (1000-2000 neurons/ml). In the microisland formed by astrocyte as well as

neurons, processes grow within the coated island but cannot reach outside because of the agarose (Figure 3).



**Figure 3. Example of the single-cell microisland of mouse hippocampal neurons.** Phase contrast micrograph of a single neuron grown for 14 days to form all of the synapses with its own dendrites.

For mass culture sterilized glass coverslips were coated with 0.2 mg/ml poly-D-lysine (PDL was dissolved in 0,1 M borate buffer; 0.05 M  $H_3BO_3$  Sigma B-0252 and 0.024 M  $Na_2B_4O_7 \times 10H_2O$  Merck A688908, pH 8.5 with HCl), approximately 200  $\mu$ l of solution were added to each coverslips. When properly cleaned (HCL 1 h,  $HNO_3$  1 h, Acetone 1 h,  $H_2O$  1 h and Ethanol 1 h), the coverslips are very hydrophilic and this small volume will spread evenly over the entire surface. After 12-24 h at room temperature (20-25  $^{\circ}C$ ), PDL solution was removed and the coverslips were rinsed several times with sterile water for 2 h each.

### 3.1.2 Hippocampal neuron preparation

Pyramidal neurons, the principal cell type in hippocampus, account for the vast majority of the total neuronal population. The hippocampus also contains a variety of interneurons, but they are comparatively few in number and most are morphologically distinguishable in culture. They form well-developed dendrites dotted with spines and make extensive, synaptically connected networks, the stage of hippocampal neuron

development in culture has been well-characterized and reasonably consistent from laboratory to laboratory (Kaech, 2006.).

Hippocampal neurons are isolated from embryonic day (E18) mice embryos. The pregnant mice were euthanized with carbon dioxide, the abdomen was cut through the abdominal wall, the fetuses were removed, decapitated and the head was transferred to a petri dish. The head was grasped firmly with a pair of forceps by inserting the tips of the forceps deeply into the orbits. Making a midline incision through the skin and skull, beginning at the level of the decapitation and continuing forward to the orbits. This tissue was reflected away to each side so that the entire cortex was revealed, the brain was removed by inserting a flat forceps of the forceps beneath the olfactory bulbs and worked them caudally, separating the nerve connections that link the brain to the skull and picking the brain up by the brainstem and transfer it to the dissecting dish.

Once the brain has been removed from the skull, it was immersed in ice-cold HBSS (Gibco-24020) at all times to prevent the tissue from drying. Under a dissecting microscope the hemispheres were removed, separating the cerebral hemispheres from the diencephalon and brainstem. With the basal aspect of the brain facing up, cut along the boundary between the diencephalons and the cerebral hemisphere. Place one blade of the scissors into the space between the hemisphere and diencephalons at the posterior pole, then cutting forward and medially around the diencephalons. Using a pair of forceps the hemispheres were spread away from the diencephalons. This procedure was repeated to remove the other hemisphere.

The outer convex border of the hippocampus, which is continuous with adjoining regions of the cortex, often is delineated by blood vessel that run along the hippocampal fissure. The inner border, which is formed by the fiber tract called the fimbria, is free. The meninges and choroids plexus were removed by stabilising the hemisphere with one pair of forceps and grasped a bit of the meninges with the other, and tug gently. Once the meninges were removed, the hippocampus was cut out, because the inner edge of the hippocampus is free and the lateral ventricle lies on its lateral aspect, only the outer edge and the anterior and posterior ends of the hippocampus were cut away from the adjoining tissue.

The hippocampi were transferred and incubated in a papain solution (1.6mM L-cysteine sigma C-7352, 250 ml DMEM Invitrogen 31966, 1 mM CaCl<sub>2</sub> Fluka 21115, 0.5 mM EDTA sigma E1644, 10 units of papain Worthington 3126 PAP) for 20 min at 37°C with gently shaking followed by incubation with inactivating solution (Albumin 2.5% (mw 238.31 mg/mol) Sigma A-4503, trypsin-inhibitor 2.5% sigma T-9253, 10 ml 10% FCS-DMEM) for 3 min. After the incubation, the tissue was dissociated by pipetting vigorously up and down, first with a 1 ml pipette (Blue tip) and second with a 200 µl pipette (yellow tip) to obtain a homogeneous solution with no obvious particles of tissue remaining. Dissociated single-cells in supernatant were transferred to fresh tubes, and cells number was determined. Approximately 1000-2000 single neurons were plated on the prepared confluent microisland astrocytes culture, and 300 single neurons/mm<sup>2</sup> were plated in the poly-D-lysine-treated coverslips, (mass culture). Cultures were incubated in NBA medium at 37°C, with 5% of carbon dioxide and 95% humidity for 14 days or longer before being used for electrophysiological recordings. To control the astrocytes overgrowth a mixture of 0.04 mM FUDR (5-Fluro-2'-deoxyuridin, sigma 0F0503, FW 246.19) and 1 mM Uridine (sigma U3003, FW 244.2) was applied for 24 hours.

### **3.2 SynaptobrevinII/VAMP2 knockout mice**

SynaptobrevinII/VAMP2 homozygous knockout mice were obtained by crossbreeding of heterozygous mice. To preserve a homogeneous genetic background we continuously crossed heterozygous mice with C57BL/6. Heterozygous mutant mice suffered no apparent morbidity or premature mortality, but homozygous mutant mice died immediately after birth. Newborn knockout mice exhibited a striking body shape, with a rounded appearance and a shoulder hump that is probably caused by excess brown fat in the upper back, but not developmental changes (Schoch et al., 2001). All experiments were performed on hippocampal neurons prepared from mice at the developmental stage E-18.

### **3.3 Genotyping**

#### **3.3.1 Genomic DNA purification**

The template DNA was obtained from the tail biopsy from embryonic mouse (3-5 mm long), the tissue were incubated at 56°C, with the 400 µl of SNET buffer (20 mM Tris-

HCl, 5 mM EDTA, 100 mM NaCl and 1% sodium dodecyl sulfate for lysis), supplemented with 8 µl proteinase K (Qiagen 19133) and shaken for several hours. The sample was centrifuged for 5 minutes at 13000 rpm and the supernatant was transferred into a fresh 2 ml tube. In order to precipitate the DNA, 400 µl isopropanol (100% Merck) was added and the sample was centrifuged at 13000 rpm for 10 minutes. After this step, a glassy pellet became visible. Supernatant was carefully removed (isopropanol pellets are more loosely attached to the side of the tube) and 400 µl of ethanol (100% Merck) was added to wash the DNA. After centrifugation at 13000 rpm for 5 minutes and removing of the ethanol, DNA pellet was dried on the shaker (37°C) for 10-20 minutes. The DNA was resuspended in 200 µl of water (Sigma) at 30°C for 1 h on the shaker, and was used for PCR was analysis.

### 3.3.2 Polymerase chain reaction

Polymerase chain reaction (PCRs) was performed to detect the gene of interest as follow:

5x Soriano buffer:

(NH <sub>4</sub> ) <sub>2</sub> SO <sub>4</sub>	83 mM
TrisHCl	335 mM
MgCl <sub>2</sub>	33.5 mM
β-mercaptoethanol	25 mM

Primers for Synaptobrevin II wild-type reaction.

Forward: Syn WT\_1      5`-GCC CAC GCC GCA GTA CCC GGA TG -3`  
 Reverse: Syn WT\_2      5`-GCG AGA AGG GCA CCC GAT GGG AG -3`

#### DNA amplification.

1x PCR reaction:

5x Soriano buffer	5 µl
DMSO	2.5 µl
dNTP 25 mM	0.5 µl
Primer Syn WT_1	0.5 µl (final concentration of 100 pM/µl)
Primer Syn WT_2	0.5 µl (final concentration of 100 pM/µl)
H <sub>2</sub> O (Sigma)	15.5 µl

Amersham Taq	0.5 µl
Genomic DNA	4 µl

PCR program:

5 min	95°C
50 s	95°C
45 s	55°C
1 min 30 s	65°C
10 min	65°C

35 cycles.

Primers for Synaptobrevin II mutant reaction.

Forward:	1910	5`-CAC CCT CAT GAT GTC CAC CAC-3`
Reverse:	1911	5`-CAG CAG ACC CAG GCC CAG GG-3`

DNA amplification

1x PCR reaction:

10x buffer	3 µl
Mg <sub>2</sub> CL 25 mM	0.5 µl
dNTP 25 mM	0.5 µl
Primer 1910	0.5 µl (final concentration of 25 pM/µl)
Primer 1911	0.5 µl (final concentration of 25 pM/µl)
H <sub>2</sub> O (Sigma)	22 µl
Sigma red Taq	1 µl
Genomic DNA	2 µl

PCR program:

5 min	94°C
30 s	94°C
1 min	60°C
2 min	72°C
10 min	72°C

40 cycles.

All primers were supplied by MWG. dNTPs were supplied from Amersham Bioscience, Sigma Red-Tag and Amersham polymerases were supplied with appropriate buffer from Sigma and Amersham Bioscience respectively.

The amplified fragments were isolated by means of electrophoresis at 120 V for 25 min in a 1.8% agarose (Healthcare Bio-science 17-0554-02) gel (0.5 µM/ml Ethidium bromide) in TAE-buffer (Tris Base 96.8g, acetic acid 22.8 ml, EDTA 0.5 mM 40 ml, double distillate water (sigma) 400ml pH 8.0), before electrophoresis the amplified fragment were supplemented with a loading dye solution (Tris-HCl 10 mM, bromophenol blue 0.03%, xylene cyanol FF 0.03%, glycerol 60%, EDTA 60 mM, pH 7.6) for easy visualization of the DNA migration during the electroforesis. The PCR products were visualized under UV light.

### **3.4 Lentivirus cloning**

cDNAs encoding for SybII and its mutants were subcloned into pRRL.sin.cPPT.CMV.WPRE lentiviral transfer vector (Follenzi et al., 2002), which contains a cPPT sequence of the pol gene and the posttranscriptional regulatory element of woodchuck hepatitis virus (Follenzi et al., 2000). To identify positive transfectants, SybII proteins were expressed as fusion constructs with the monomeric red fluorescent protein (mRFP) protein linked to the C-terminal, intravesicular domain of SybII. According to the protocol from Kesavan et al., the following amino acids (underlined) were inserted into the juxtamembrane region of SybII: 4aa, KNKLGGKL; 5aa: KNKLGGSKL, 6aa: KNKLGGSGKL, 7aa: KNKLGGSGGKL, 8aa: KNKLGGSGGSKL, 11aa: KNKLGGSGGSGSKL. The KL sites, flanking the GGS motif, encode for HindIII restriction sites and were generated to allow a primer-based elongation of the inserted amino acid-stretch in order to facilitate the cloning process. Constructs were verified by DNA sequence analysis. All mutants were produced and kindly provided by my doctoral college Yvonne N. Schwarz.

#### **3.4.1 Lentiviral production and transfection**

The transfer vector plasmid and the helper plasmids were transfected into human embryonic kidney HEK293T cell line using Lipofectamine 2000 according to a modified Invitrogen protocol. Briefly, after 14 hours, the transfection medium was replaced with OptiMEM, 10% FCS and 100mM sodium pyruvate and 48 hours later

the virus was harvested, filtered (0.4  $\mu\text{m}$  PVDF membrane, Millipore) and concentrated using a centrifugal filter device (100kDa molecular weight cutoff; Amicon Ultra-15; Millipore, Bedford MA). The viral particles were immediately frozen and stored at  $-80^{\circ}\text{C}$ . For each virus, a titer test on neuronal cultures was performed to adjust the number of infectious units to a transfection efficacy of higher than 80 %. Neurons were transfected at day 1 *in vitro* by adding 100-300  $\mu\text{l}$  viral suspension to the culture medium.

### 3.5 Electrophysiology

Synaptic responses were recorded from hippocampal autaptic neuron, after 14-17 days in culture. All electrophysiological experiments were carried out at room temperature  $22-24^{\circ}\text{C}$  in standard extracellular medium contained 130 mM NaCl, 2.4 mM KCl, 10 mM HEPES, 10 mM glucose, 4 mM  $\text{CaCl}_2$ , 4 mM  $\text{MgCl}_2$ , 10 mM  $\text{NaHCO}_3$ , the osmolarity was 300-310 mOsm, (pH 7.3). 1  $\mu\text{M}$  of tetrodotoxin (Sigma T-5651) was added to the extracellular medium for mass culture to avoid spontaneous action potential. For each experiment, approximately equal numbers of cells were measured in parallel on the same day *in vitro*. The intracellular solution contained the following; 137 mM K-gluconate, 11 mM NaCl, 2 mM MgATP, 0.3  $\text{Na}_2\text{GTP}$ , 1.1 mM EGTA, 11 mM HEPES, 11 mM D-glucose, pH 7.3, osmolarity 300 mOsm. For glutamate antagonis experiments, 200  $\mu\text{M}$  of  $\gamma$ -D-glutamylglycine ( $\gamma$ -DGG) (Tocris Cookson, Ellisville, MO 0112) was bath applied using a fast perfusion system. To minimize the potential contribution of GABAergic currents the reversal potential of chloride-mediated currents was adjusted to the holding potential.

The patch pipettes were prepared using a horizontal puller (Sutter of instrument, model p-87, Novato, USA) from glass capillaries (Type GC159 F-10, Harvard apparatus) with an open tip resistance about 3.5-4.5  $\text{M}\Omega$  in chloride based internal solution.

Cells were whole-cell voltage clamped at  $-70$  mV with an EPC 10 patch clamp amplifier (Heka elektronik) under control of Pulse 8.5 program (HEKA Elektronik), Current were bassel filtered at 2.9 kHz (four pole Bessel filter EPC10) and digitised at a rate of 50 kHz. The series resistance was compensated to 80-85%, only cells with resistances below 10  $\text{M}\Omega$  were analysed.

To determine the mEPSC properties with reasonable fidelity, spontaneous events with a peak amplitude  $>15$  pA ( $\sim 5$  times the S.D. of the background noise, e.g. SybII:  $3.2 \pm 0.08$  pA, 11aa:  $3.05 \pm 0.09$  pA) and a charge criterion  $>30$  fC were analysed using a commercial software (Mini analysis, Synaptosoft, Version 6.0.3). The mEPSC decay was fitted with double exponential.

### **3.6 Stimulations Protocols**

#### **3.6.1 Action potential evoked signals**

EPSC were evoked by depolarizing the cell (micro-islands containing one transfected neuron) from  $-70$  to  $+10$  mV for  $0.7$  ms at low frequency stimulation ( $0.2$  Hz). The magnitude of the responses was quantified by measuring amplitude as well as the integral of the resulting EPSC.

#### **3.6.2 Osmotic stimulation and release probability**

A pool of readily releasable pool has been defined for hippocampal synapses (Stevens and Tsujimoto, 1995). This pool consists of about 12 quanta per synapse, and replenishing takes about 10 s when it has been completely depleted. One method used for defining the readily releasable pool is applying hypertonic solution. (Rosenmund and Stevens, 1996).

The RRP at hippocampal synapses was defined by a 5 sec application of 500 mM Sucrose (standard extracellular medium containing 500 mM of Sucrose) to the entire microisland. During the application of the hypertonic solution, the quantal release rate jumps rapidly to relative high level and then declines approximately exponentially to a low steady level, the integral of the transient component after subtraction of steady state component give the total charge of RRP (Figure 4).

To calculate the release probability (RP), 0.5 Osm hypertonic solutions was applied for 5 s, after 5 s evoked action potential (Figure 4). The RP was calculated as the charge released by action potential divided by the total charge released by application of the hypertonic solution.

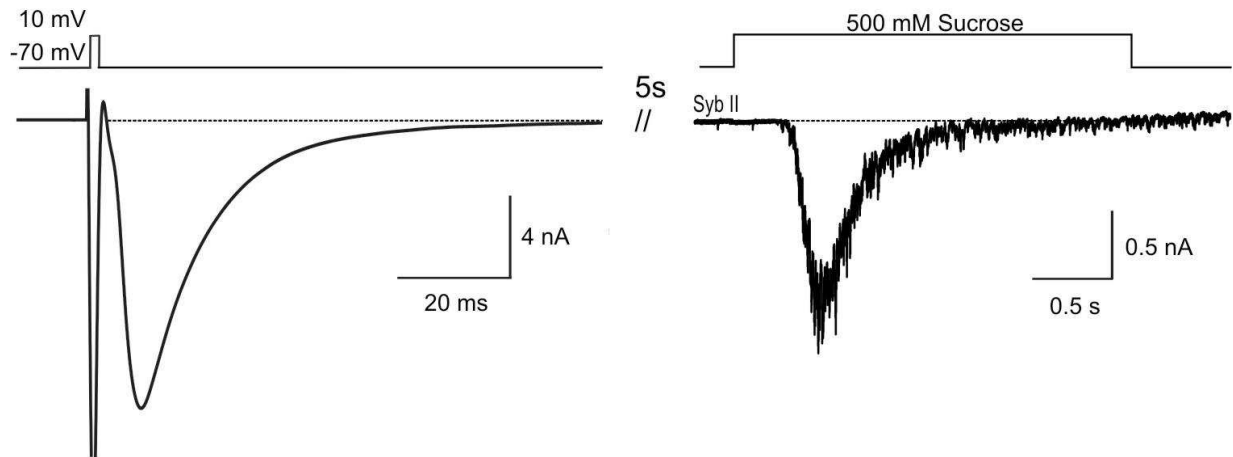


**Figure 4. Osmotic stimulation and release probability calculation.** Left, excitatory postsynaptic current (EPSC) induced by a brief depolarisation from a holding potential of  $-70$  mV to  $+10$  mV for  $0.7$  ms duration time. Right, Hypertonic solution-evoked response using ( $500$  mM sucrose) a fast perfusion system for  $5$  s duration time. The total charge of the transient inward current generated during this stimulation protocol is typically defined as readily releasable pool (RRP) (Rosenmund and Stevens, 1996). The charge of the area under the curve of EPSC divided by the charge of RRP gives the release probability.

### 3.7 Statistical analyses

Values are given as mean  $\pm$  s.e.m.. To determine statistically significant differences, one-way analysis of variance and a Tukey-Kramer post-test for comparing groups were used, if not indicated otherwise.

## 4. Results

### 4.1 SynaptobrevinII-mRFP fully rescues synaptic transmission in Synaptobrevin deficient neurons

Using autaptic hippocampal neurons (Bekkers and Stevens 1991) from SybII deficient mouse embryos, we expressed exogenous SybII protein using a lentiviral expression system (Invitrogen). Expression of SybII-mRFP (SybII) successfully rescues the action potential evoked response in knockout neurons (Figure 5). Thus, these results make SybII ko neurons a useful cell model, in which different mutant v-SNARE proteins can be expressed and studied on a zero v-SNARE background.

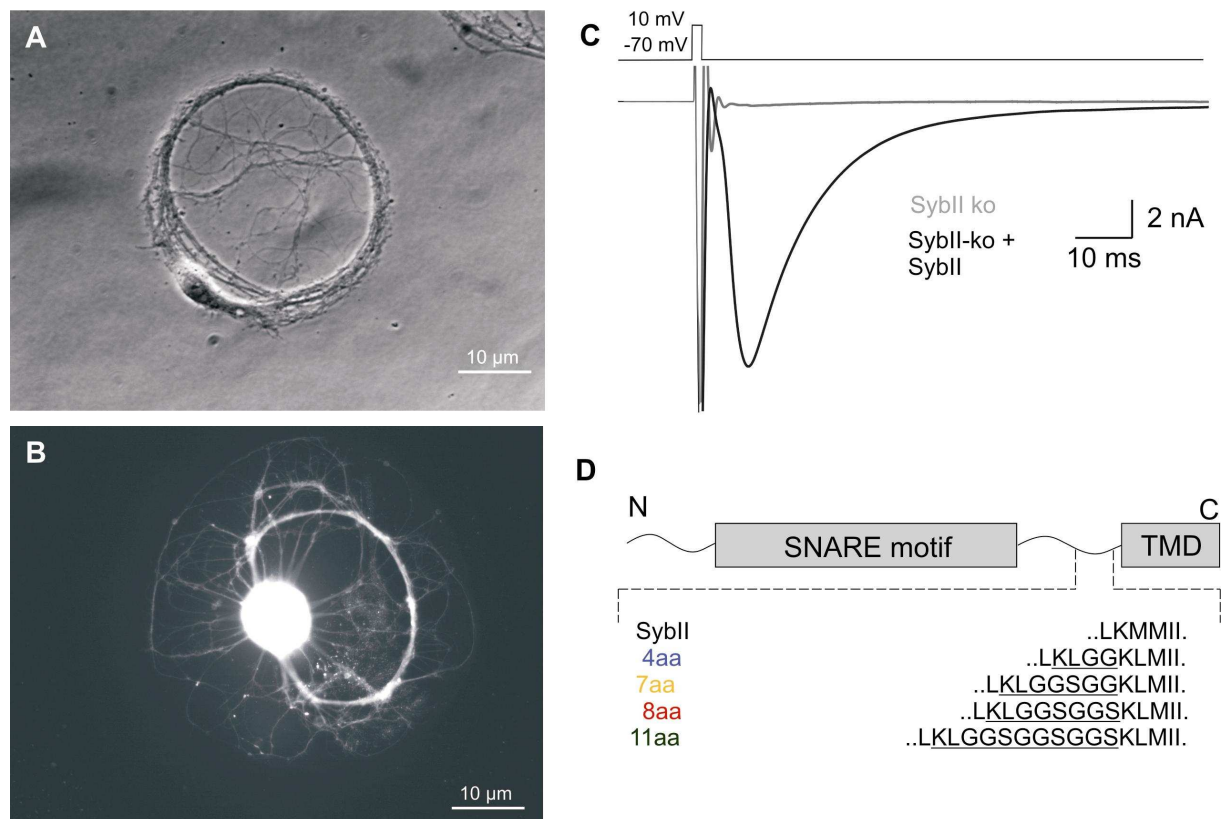


**Figure 5. Rescue of the action potential evoked response in SybII ko neurons and schematic view of SybII domains.** A) Autaptic culture of SybII ko neuron cultured on a glial microisland. B) SybII ko neuron (14DIV) transfected with SybII-mRFP virus one day after plating. C) Action potential (AP) evoked response is abolished in Sybko neurons, but can be rescued by expression of SybII-mRFP. D) Schematic view of SybII domain, SNARE motif and transmembrane domain (TMD) are boxed. Underlined amino acid sequences show the insertions between SNARE domain and TMD.

## 4.2 SynaptobrevinII-mRFP knockin neurons exhibit similar exocytotic responses when compared with wild type neurons

The former result that SybII, C-terminally tagged with the mRFP, efficiently restores neurotransmitter release was a prerequisite for the generation of a new knockin mouse strain that expresses SybII-mRFP. In collaboration with the lab of Prof. Dr. Jens Rettig we comparatively analyzed the secretory responses mediated by SybII and its fluorescent variant. Action potential evoked responses and release in response to hypertonic sucrose application recorded from autaptic neurons expressing SybII-mRFP (SybII-mRFP<sub>in</sub>) were indistinguishable from those measured from wild type neurons (SybII-wt, Figure 6A). Furthermore, synaptic parameters like time to peak and release probability were not significantly altered (Figure 6B), confirming that mRFP fused to the C-terminus of the protein does not interfere with SynaptobrevinII function during exocytosis.

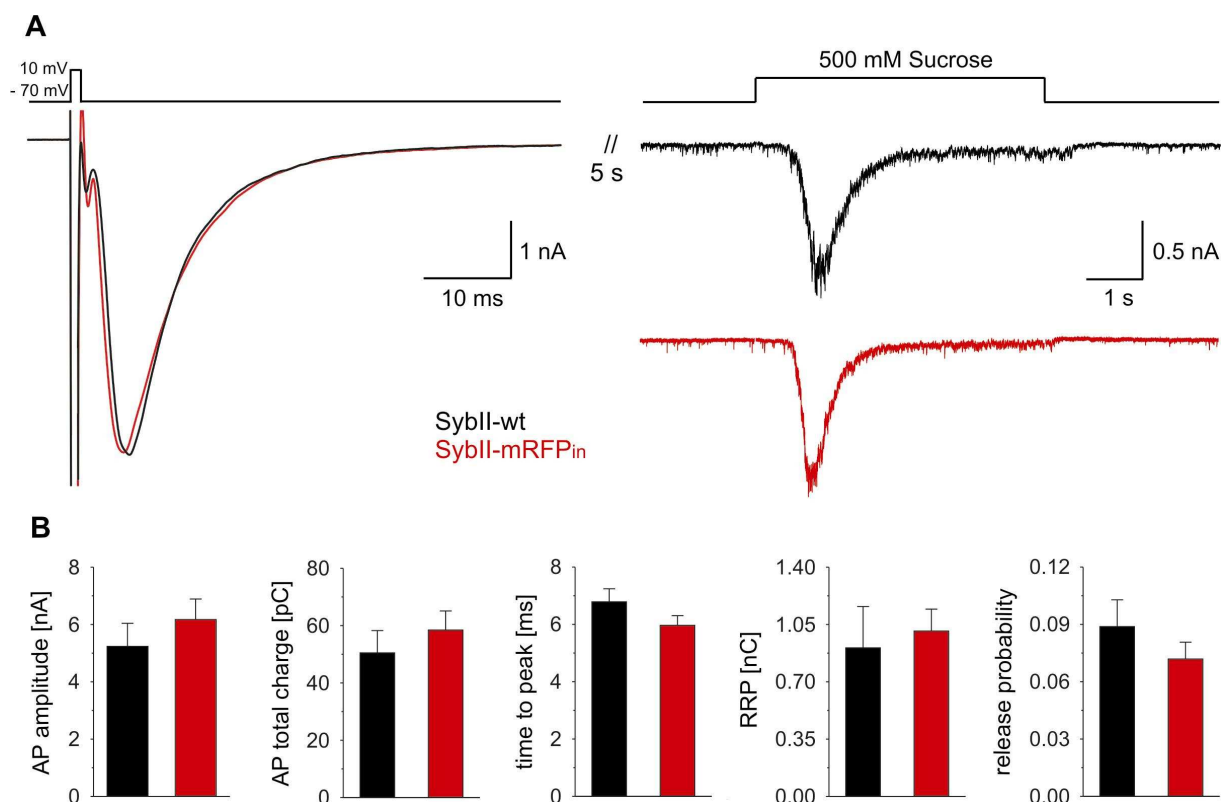


**Figure 6. SynaptobrevinII-mRFP knockin neurons show similar exocytotic responses than neurons expressing SynaptobrevinII.** A) Action potential evoked response and readily releasable pool measured from SybII-wt neurons were not different from those recorded from SybII-mRFP<sub>in</sub> neurons B) Average synaptic parameters do not show significant differences between SybII-wt and SybII-mRFP<sub>in</sub> neurons. SybII-wt, n=20; SybII-mRFP<sub>in</sub>, n=20, (paired student's t-test p>0.05).

### 4.3 Increasing the distance between the SNARE motif and the TMD of SybII gradually reduces evoked transmitter release

First, we characterized how extending the juxtamembrane region of SybII affects neurotransmitter release in response to a single action potential. SybII ko neurons were infected with lentiviral expression constructs encoding for SybII or its variants that carry amino acid insertions of different lengths in the juxtamembrane region of the protein (Figure 6).

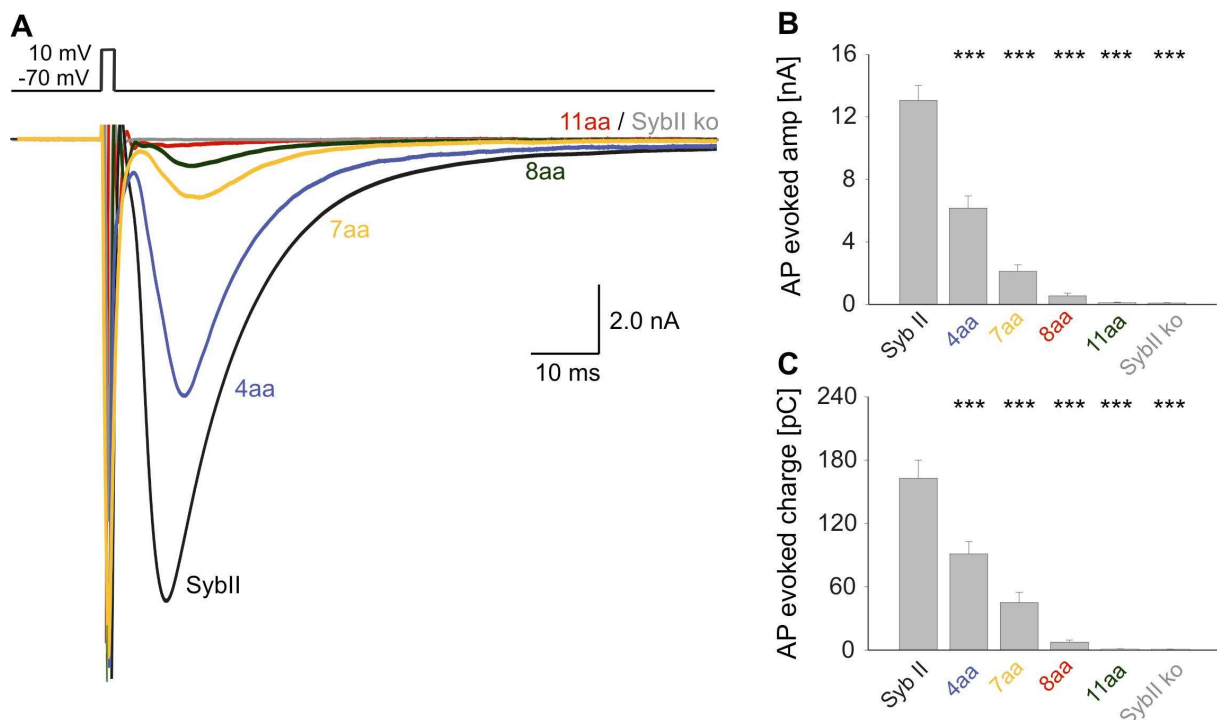


**Figure 7. Extending SybII's juxtamembrane region decreases evoked neurotransmitter release in a linker-length dependent fashion.** A) Averaged responses of action potential evoked release from SybII ko neurons expressing SybII or its variants. B) Amplitude and C) charge of the AP evoked signals decrease with increasing linker length. (SybII; n = 16, 4aa; n = 20, 7aa; n = 19, 8aa; n = 14, 11aa; n = 10. \*\*\*p<0.001, one-way analysis of variance).

Compared with SybII wild-type protein, the insertion of a 4 amino acid linker strongly reduces the amplitude of the action potential evoked response by 54 %. Increasing the length of the linker to 7, 8 and 11 amino acids further decrease the amplitude of the evoked signal (Figure 7A and 7B). With the 11aa insertion the evoked signals are nearly abolished and indistinguishable from those measured in knockout neurons (Figure 7, red trace). For the evoked EPSC charge, a similar linker length dependent depression in release is observed (Figure 7C). Thus, amino acid insertions

immediately preceding the TMD gradually decrease the action potential evoked EPSC.

#### 4.4 v-SNARE linker mutants alter exocytosis timing

To test whether linker mutants affect exocytosis beyond priming of SSVs, we determined the stimulus-secretion coupling in response to single action potentials for wild type and mutant proteins. As shown in Figure 8A, the synaptic delay is progressively prolonged with increasing the linker's length. On average, exocytosis initiation of SSVs carrying a mutant protein occurs with a significant time lag (SybII:  $2.33 \pm 0.17$  ms; 4aa:  $3.12 \pm 0.22$  ms; 7aa:  $3.91 \pm 0.22$  ms; 8aa:  $4.77 \pm 0.37$  ms, Figure 8B). Furthermore, within the single groups, we were not able to detect any correlation between EPSC amplitude and the synaptic delay. However, beyond the groups synaptic delay exhibited a close correlation with EPSC amplitude (Figure 9), indicating that the amplitude of the EPSC is not a determinant for synaptic delay. Each increase in linker size also caused a progressive increase in the time to peak measured from the end of the stimulus to the maximum of the synaptic response (Figure 8C).

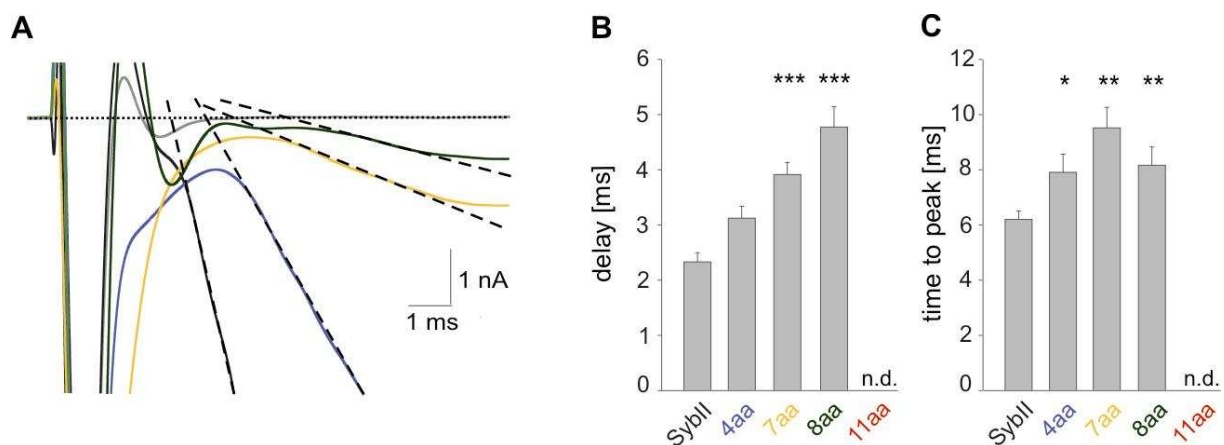


**Figure 8. v-SNARE linker mutants alter exocytosis timing.** A) Amino acid insertions delay the onset of release. B) Average synaptic delay, SSVs carrying a mutant protein exocytose with a significant time lag. C) Time to peak was calculated from the end of the stimulus to the maximum of the synaptic response. (Syb II; n = 16, 4aa; n = 20, 7aa; n = 19, 8aa; n = 14, 11aa; n = 10. \*p<0.05, \*\*p<0.01, \*\*\*p<0.001, one-way analysis of variance).

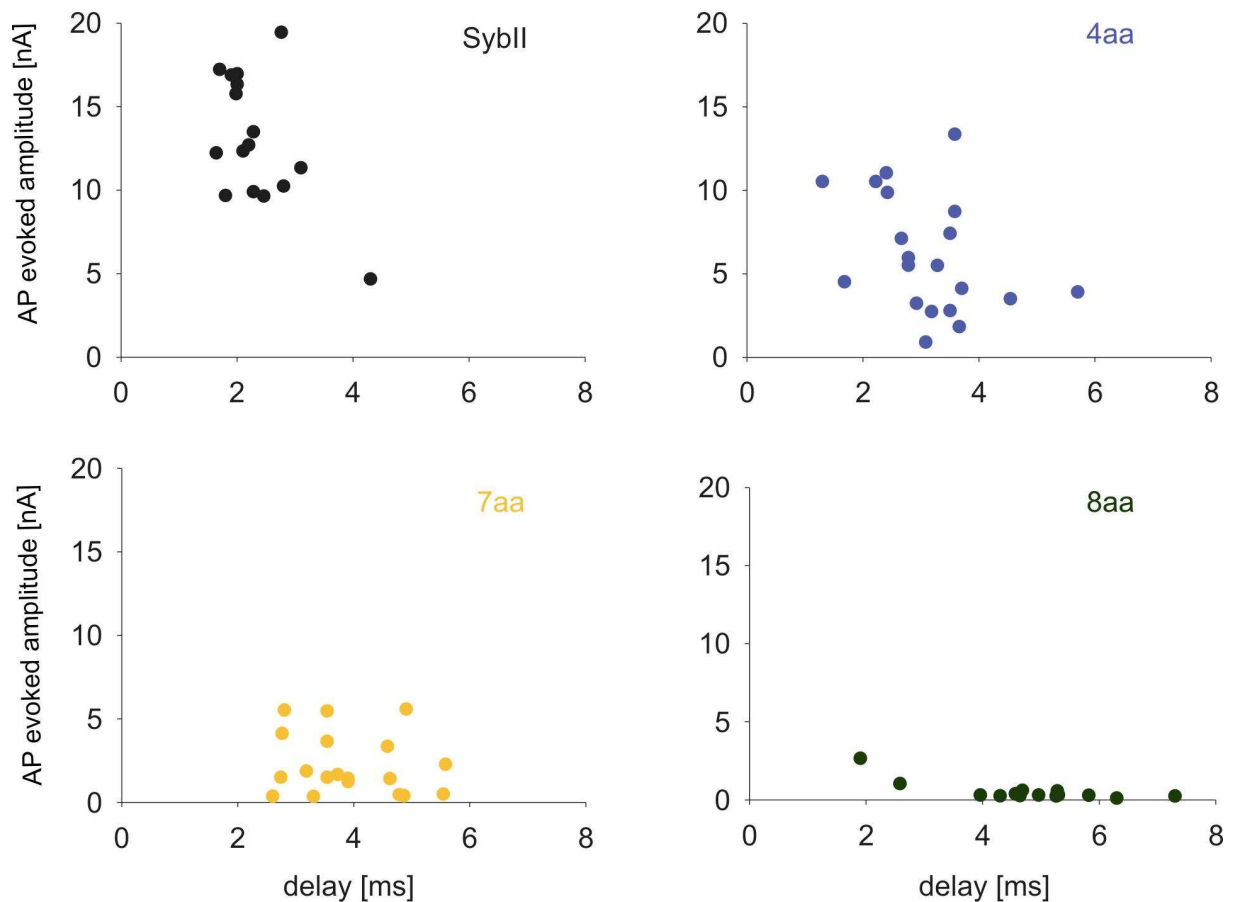


**Figure 9. Synaptic delay.** Note that the synaptic delay does not exhibit any correlation with EPSC amplitude within the single groups. Such correlation is evident beyond the groups (Syb II; n = 16, 4aa; n= 20, 7aa; n = 19, 8aa; n = 14, 11aa; n = 10).

To further analyse the kinetics of neurotransmitter release, we integrated the EPSC over time. The cumulative charge plot is well approximated with a sum of two exponential functions (Figure 10A). In neurons expressing the linker mutants, the time constant of the first synchronous component was significantly slower than that observed with the wild type protein (Figure 10B). Similar differences between wild type and mutant protein are observed for the time constant of the slow asynchronous component of release (Figure 10C). Furthermore, both components of the synaptic response decrease in magnitude with increasing linker length, albeit the synchronous phase shows a higher sensitivity than the asynchronous phase (Figure 10D and 10E). Taken together, these data indicate that a tight molecular link between the complex-forming SNARE motif and the TMD of SybII controls the time course of the synaptic response suggesting a postpriming function of v-SNARE proteins during SSV exocytosis.

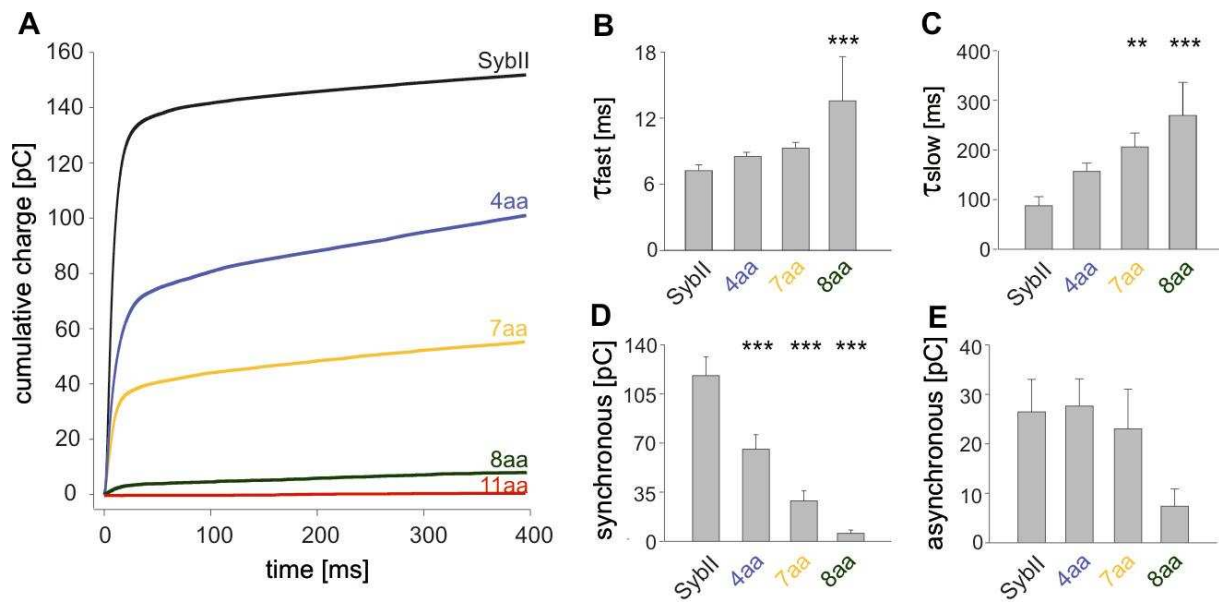


**Figure 10. Kinetic analysis of action potential evoked response.** A) Cumulative charge plot is well approximated with a sum of two exponential functions. (B and C) Time constants of the synchronous and asynchronous release. (D and E) Fast synchronous and slow asynchronous components respectively. Note that both components of release response decrease in magnitude with increasing linker length, albeit the first phase shows a higher sensitivity than the second phase. (SybII;  $n = 12$ , 4aa;  $n = 17$ , 7aa;  $n = 15$ , 8aa;  $n = 5$ .  $**p < 0.01$ ,  $***p < 0.001$ , one-way analysis of variance).

#### 4.5 Expression of v-SNARE proteins and synaptogenesis do not change with linker mutations

We next analysed the expression levels of the v-SNARE variants and whether they support synapse formation to the same degree as the wild type protein. Immunostaining with an antibody directed against SybII's N-terminus shows that mutant proteins do not differ from the wild type protein regarding level or pattern of protein expression in SybII knockout neurons (Figure 11A and 11B). The similar dotted appearance of the immunosignals indicates correct sorting of the mutant protein to synapses (Figure 11A and 11B insets). Immunolabeling of the vesicular marker protein Synaptophysin shows that SybII-ko neurons exhibit the same synapse density as wild type cells. Furthermore, expression of SybII or its mutant variants in SybII-ko neurons leaves the synapse number unchanged (Figure 11C), indicating that linker mutations do not interfere with synaptogenesis. Thus, neither variations in protein expression (or sorting) nor deficiencies in synapse formation can be held responsible for the phenotype of the mutant protein.

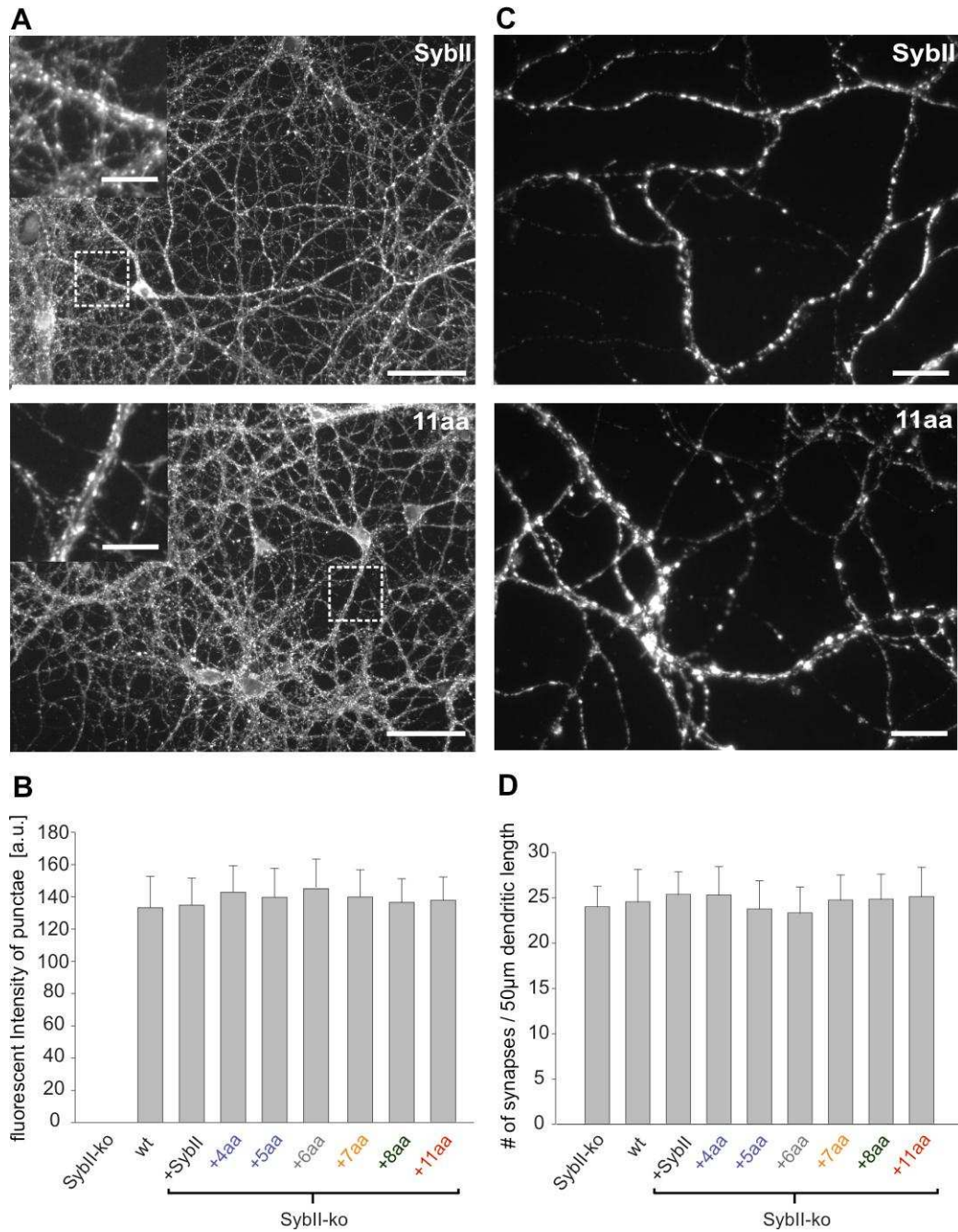


**Figure 11. Expression of v-SNARE proteins and synaptogenesis do not change with linker mutations** (A) Exemplary images of SybII ko neurons expressing SybII wild type or SybII 11aa. Immunosignals (FITC channel) were detected with an affinity-purified monoclonal antibody (69.1) directed against the N-terminus of SybII. B) Mean intensity of puncta was measured from 50µm stretches of an axon. In SybII ko neurons signals were not detectable. C) Exemplary images of SybII and SybII 11aa expressing neurons stained for the vesicular marker protein Synaptophysin. D) Quantitative assessment of synapses per 30µm axon length shows that the synapse density was not altered in SybII ko neurons expressing SybII wild type and mutant proteins. (SybII; n= 25, 4aa; n= 26, 5aa; n= 24, 7aa; n= 20, 8aa; n= 22, 11aa; n= 24)

#### **4.6 Readily releasable pool size and release probability decrease with increasing linker length**

Important physiological factors that might contribute to the defect in the size of the action potential evoked response mediated by the mutant proteins are the size of the readily releasable pool (RRP) of synaptic vesicles and the release probability (RP). Only a fraction of synaptic vesicles in close proximity to the active zone are primed and constitute the readily releasable pool (RRP) (Rizzoli and Betz, 2005). This pool consists of about 12 quanta per synapse, and when the pool has been completely depleted, replenishing takes about 10 s in hippocampal synapses. One method used for defining the RRP is by application of hypertonic solution for several seconds. When a hypertonic solution is applied, the quantal release rate jumps rapidly to a relatively high level and then declines exponentially to a low, steady level. The integral of the transient inward current produced by the concomitant release of glutamate provides a direct estimate on the number of vesicles within the RRP (Rosenmund and Stevens, 1996). As shown in Figure 12A and 12B, the size of the RRP significantly and systematically decreases with lengthening of SybII's juxtamembrane region, indicating that linker mutations interfere with the establishment or maintenance of the release-ready state.

To further elucidate reasons for the reduced EPSC with the SybII mutant proteins, we analysed the vesicular release probability in response to single action potential stimulation. The ratio of charges evoked by an action potential and that during subsequent sucrose stimulation provides an estimate on the release probability (Figure 4). Indeed, the release probability decreases with longer amino acid insertions (Figure 12C). Given that SSVs experience only a transient  $\text{Ca}^{2+}$  rise during an action potential, it is conceivable that the reduced RP observed for the mutant proteins might be a consequence of the synaptic delay. In fact, a negative correlation is evident when we plot RP vs synaptic delay for all mutants, supporting the idea that SSVs carrying mutant proteins slowly react at the moment of  $\text{Ca}^{2+}$  rise (Figure 12D). Thus, this observation reinforces the view that a short intramolecular distance between the SNARE motif and the TMD of the v-SNARE protein regulates  $\text{Ca}^{2+}$ -triggered exocytosis at a postpriming level.

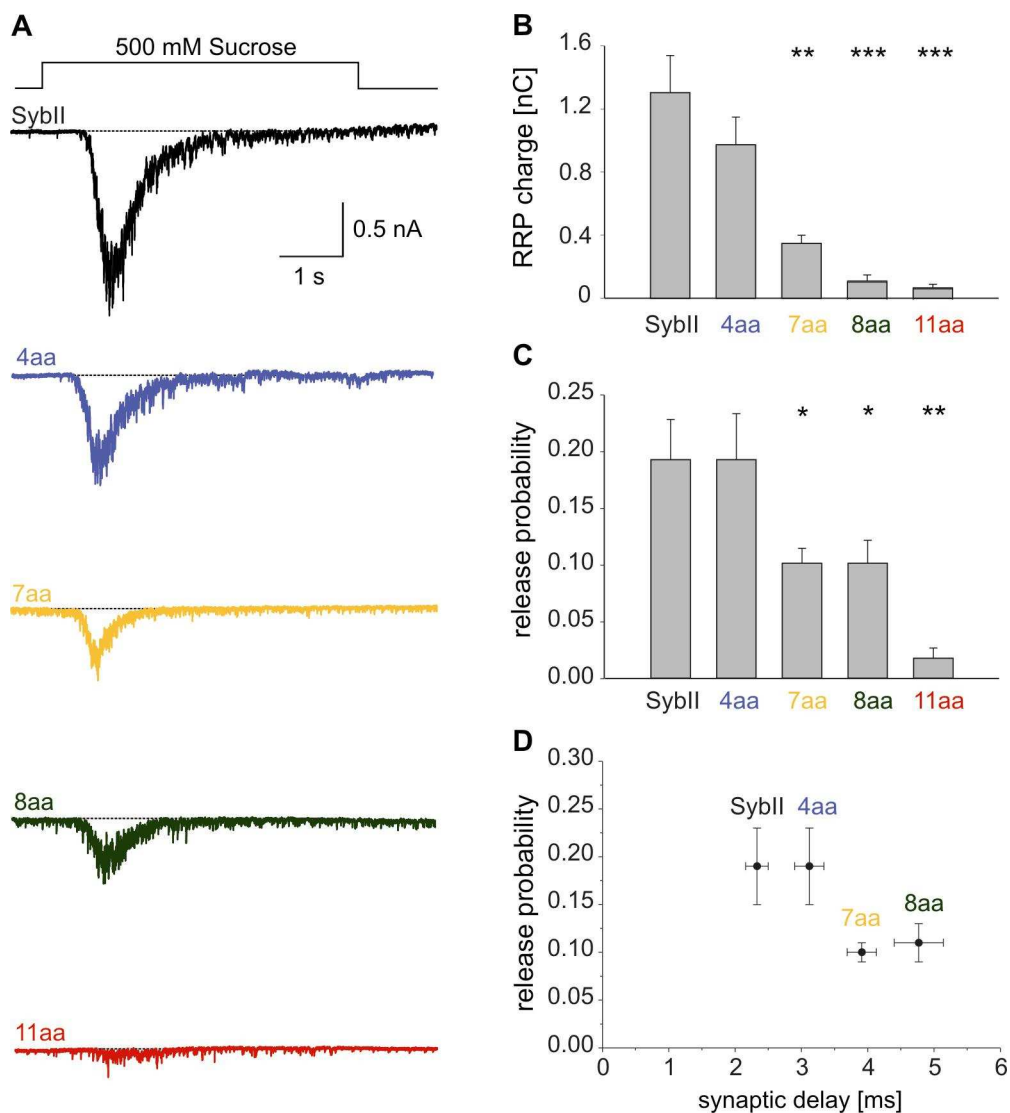


**Figure 12. Readily releasable pool size and release probability decrease with increasing linker length.** A) Exemplary traces of stimulated sucrose release of SybII ko neurons expressing SybII or its mutated variants (B and C) The readily releasable pool (RRP) size and the release probability (RP) are sensitive to extension of the juxtamembrane region of SybII D) Reduction in the release probability might be caused by the delay in exocytosis initiation. (SybII; n = 12, 4aa; n= 20, 7aa; n = 17, 8aa; n = 14, 11aa; n = 10. \* $p < 0.05$ , \*\* $p < 0.01$ , \*\*\* $p < 0.001$ , (one-way analysis of variance).

#### 4.7 SybII action underlies the speeding in mEPSC time course

To test whether the distance between the complex-forming SNARE domain and the TMD of Synaptobrevin is critical for quantal signaling, we measured spontaneous excitatory postsynaptic currents (mEPSC) in the presence of  $1\mu\text{M}$  TTX using mass cultures of hippocampal neurons. As shown in Figure 13, expression of the 11aa mutant in SybII ko neurons changes not only the frequency of spontaneous events

(SybII:  $7.3 \pm 1.3$  Hz,  $n=34$ , 11aa:  $2.9 \pm 0.6$  Hz,  $n=22$ ,  $P = 0.014$ ) but also reduces their amplitude. On average, the mean amplitude of 11aa mediated mEPSCs is  $\sim 1.4$  fold smaller than that of SybII-signals (SybII:  $50.4 \pm 2.4$  pA,  $n=34$ , 11aa:  $37.0 \pm 1.6$  pA,  $n=22$ ). A comparison of averaged miniature events, aligned to the midpoint of the rise time, illustrates the reduced amplitude and the slower time course of 11aa-mediated events compared with SybII-mediated signals (Figure 13B,C).

The decay phase of averaged SybII mEPSCs (Figure 13B,C) is best approximated by a sum of two exponentials revealing an initial fast ( $\tau_{\text{fast}}$ ) and a subsequent slower component ( $\tau_{\text{slow}}$ ) of decay ( $A_{\text{fast}} -24.7 \pm 2.1$  pA,  $\tau_{\text{fast}} 0.45 \pm 0.02$  ms,  $A_{\text{slow}} -17.4 \pm 1.1$  pA,  $\tau_{\text{slow}} 2.42 \pm 0.7$  ms,  $n=19$ ). The slow component is not mediated by NMDA receptors since extracellular solutions contained  $\text{Mg}^{2+}$  and were nominally glycine free to block NMDA receptor mediated responses. In comparison to SybII, the initial phase of 11aa mEPSC is characterized by both a significant lower amplitude ( $A_f - 17.2 \pm 1.1$  pA,  $n=16$ , Figure 13D) and slower time course ( $\tau_{\text{fast}} 0.79 \pm 0.05$  ms). The second component instead retains a nearly unchanged amplitude ( $A_{\text{slow}} -14.8 \pm 1.3$  pA) with a slower decay ( $\tau_{\text{slow}} 3.13 \pm 0.12$  ms,  $n=16$ , Figure 13D). To obtain similar speed clamp, the resistance series compensation was adjusted to the same value in both groups (Figure 13E). Furthermore, we calculated the “false” event rate ( $\lambda_f$ ), based on random noise, which is given by  $\lambda_f = f_c e^{-\theta^2/2rms^2}$  (Colquhoun and Sigworth, 1995). For nearly identical baseline noise ( $rms$ ) of about 3.0 pA/ms in SybII and mutant recordings (Figure 13F), a threshold ( $\theta$ ) of 15 pA/ms and an effective bandwidth ( $f_c$ ) of 2.9 kHz, the false event rate is 0.01 Hz representing less than one hundredth of the observed frequency. These results show that properties of the release process rather than experimental inconsistencies like overcompensation of the clamp or detection of false signals are responsible for the observed differences in mEPSC time course. Taken together, the linker mutant protein diminishes the peak amplitude and slows the decay of the mEPSC

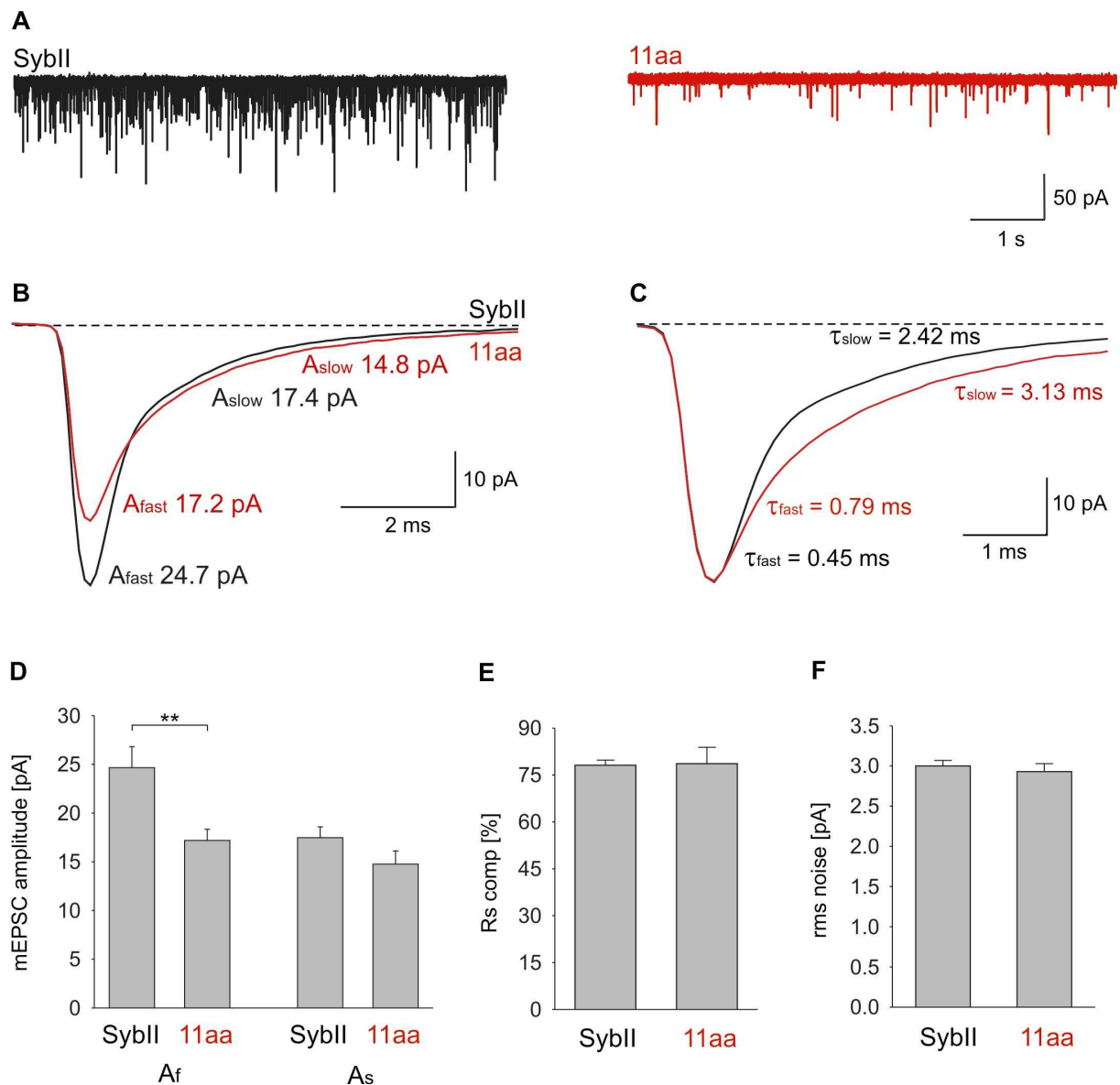


**Figure 13. Quantal signaling is altered by linker mutations** A) Representative traces of spontaneous miniature excitatory postsynaptic current mEPSC of SybII knockout neurons (mass culture) expressing SybII or SybII carrying 11aa insertion in presence of 1 mM of TTX. B) Averaged mEPSCs with similar charge taken from SybII ko neurons expressing SybII wild type protein (black) or 11aa insertion (red). C) Superimposed normalized averages. SybII events exhibit a faster release time course than 11aa as is shown by the decay time constant, which was calculated by fitting the average mEPSCs using a double exponential function. D) Bar graph showing that the linker mutant protein affects preferentially the magnitude of the fast component of the mEPSC. E and F) Resistance series compensation and rms noise where comparable between SybII and mutant protein. (SybII: n=23, 11aa: n=16 cells, \*\*p<0.01, one-way analysis of variance).

A comparison of the histogram frequency distributions as well as cumulative frequency of the quantal parameters shows that the amplitude distribution of 11 amino acids mediated mEPSCs is shifted to lower values without changing the quantal charge (Figure 14).  $\tau$  values from single exponential fits to the individual

responses ( $\tau_{\text{single}}$ ) confirm the significant difference between the decays of SybII and 11aa signals (SybII  $1.20 \pm 0.06$  ms, 11aa  $1.87 \pm 0.09$ ,  $P < 0.001$ ) (Figure 15).

The 10-90% rise time of quantal signals differs for rise times longer than 300  $\mu\text{s}$ , but is unchanged for more rapidly rising signals, most likely due to the limiting response time of the cell-electrode system. To minimize the contribution of quantal events from release sites distant to the soma, we restricted our analysis to signals with rise times faster than 400  $\mu\text{s}$ , comprising about 50% of the recorded events. Notably, the relative changes in  $\tau_{\text{single}}$  between the mutant and the SybII signals are preserved, indicating that experimental inconsistencies like variable dendritic filtering cannot account for the observed differences (events  $> 15$  pA,  $\tau_{\text{singleSybII}} / \tau_{\text{singlemut}}$ : 0.64; events  $rt < 400$   $\mu\text{s}$ ,  $\tau_{\text{singleSybII}} / \tau_{\text{singlemut}}$ : 0.65, Figure 15A). The same result is obtained for the peak amplitude (events  $> 15$  pA,  $A_{\text{SybII}} / A_{\text{mut}}$ : 1.36, events  $rt < 400$   $\mu\text{s}$ ,  $A_{\text{SybII}} / A_{\text{mut}}$ : 1.40, Figure 15B).

Since quantal signals vary greatly with respect to their magnitude, we analysed the effect of the mutant protein on differentially sized events. As shown in Figure 16A, the event's amplitude scales proportionally to the event's charge (slope 0.52 pA/fC,  $r^2=0.99$ , Figure 16B) and is significantly reduced over the entire range of charges for 11aa signals (slope 0.34 pA/fC,  $r^2=0.99$ , Figure 16B). In the same line, the kinetic parameters like 10-90% rise time and  $\tau_{\text{decay}}$  are shifted to longer times for the mutant protein when compared with SybII signals (Figure. 16C and 16D). Thus, alterations in magnitude and time course of the mutant signals are independent of quantal charge and affect small and large events to the same degree.

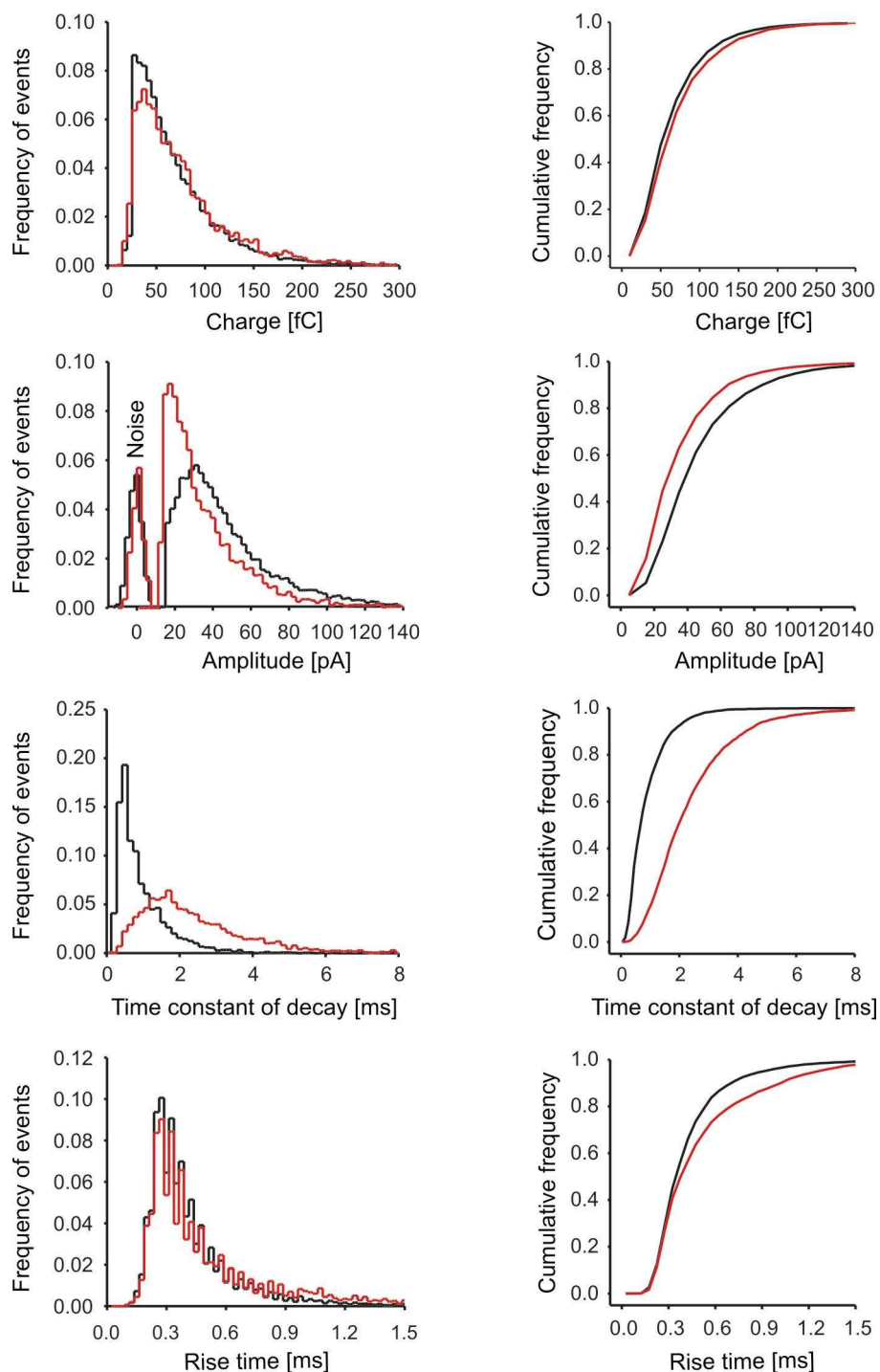


**Figure 14. Comparison of the frequency distributions of quantal signals by the SybII or the 11aa insertion.** Properties of mEPSC mediated by SybII (black,  $n=15293$ ), 11aa (red,  $n=3829$ ) displayed as histogram frequency and cumulative frequency distribution for the indicated parameters. Visualization of the cumulative frequency distribution of quantal events from this reciprocal pairs reveals a rightward shift in the amplitude and leftward shift in the rise time as well as the time constant of decay in the quantal events mediated by 11aa insertion relative to the control (SybII). Background noise distribution (peak centred at 0 pA) was obtained from 10-20 ms of recordings in which no mEPSC were evident.

The combined set of data for different insertion mutants reveals a linker-length-dependent attenuation of the mEPSC amplitude that is accompanied with a strong and significant prolongation of the event's  $\tau_{\text{slow}}$  and  $\tau_{\text{fast}}$  (Figure 17). These results show that v-SNARE action underlies the speeding in mEPSC time course. An attractive scenario could be that a tight coupling between SNARE domain and TMD of SybII is required for rapid transmitter discharge from small synaptic vesicles shaping the entire mEPSC signal.

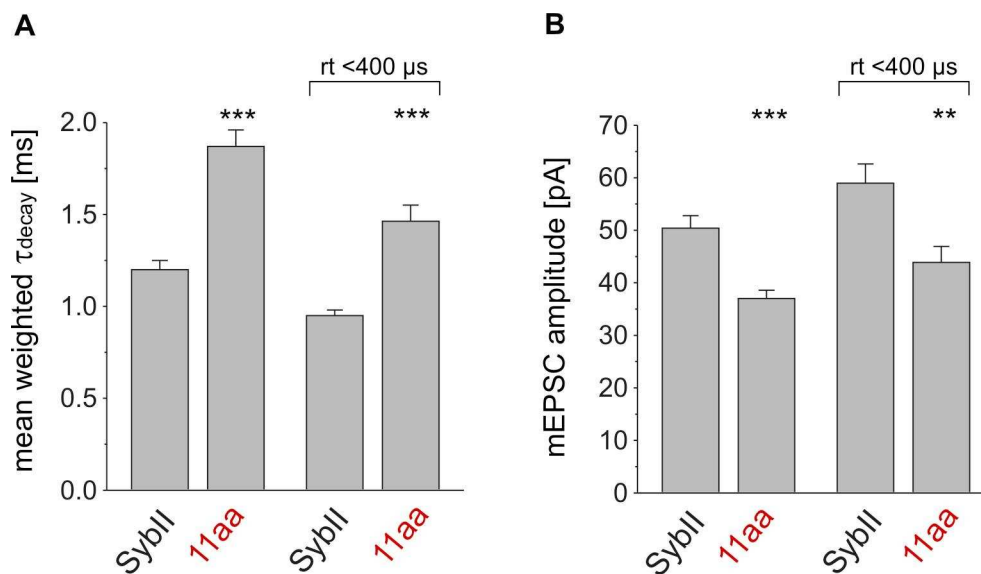


**Figure 15. Variable electrotonic filtering cannot account for the differences in the mEPSC time course.** SybII (n=19 cells) and 11aa insertion (n=16 cells). Note that the relative changes in  $\tau_{\text{decay}}$ , (A) as well as in the amplitude, (B) of SybII- and mutant signals are preserved when the analysis is restricted to events with rise times faster than 400  $\mu$ s to minimize the signal's electrotonic distortion. (\*\*p=0.005, \*\*\*p<0.001, one-way analysis of variance)

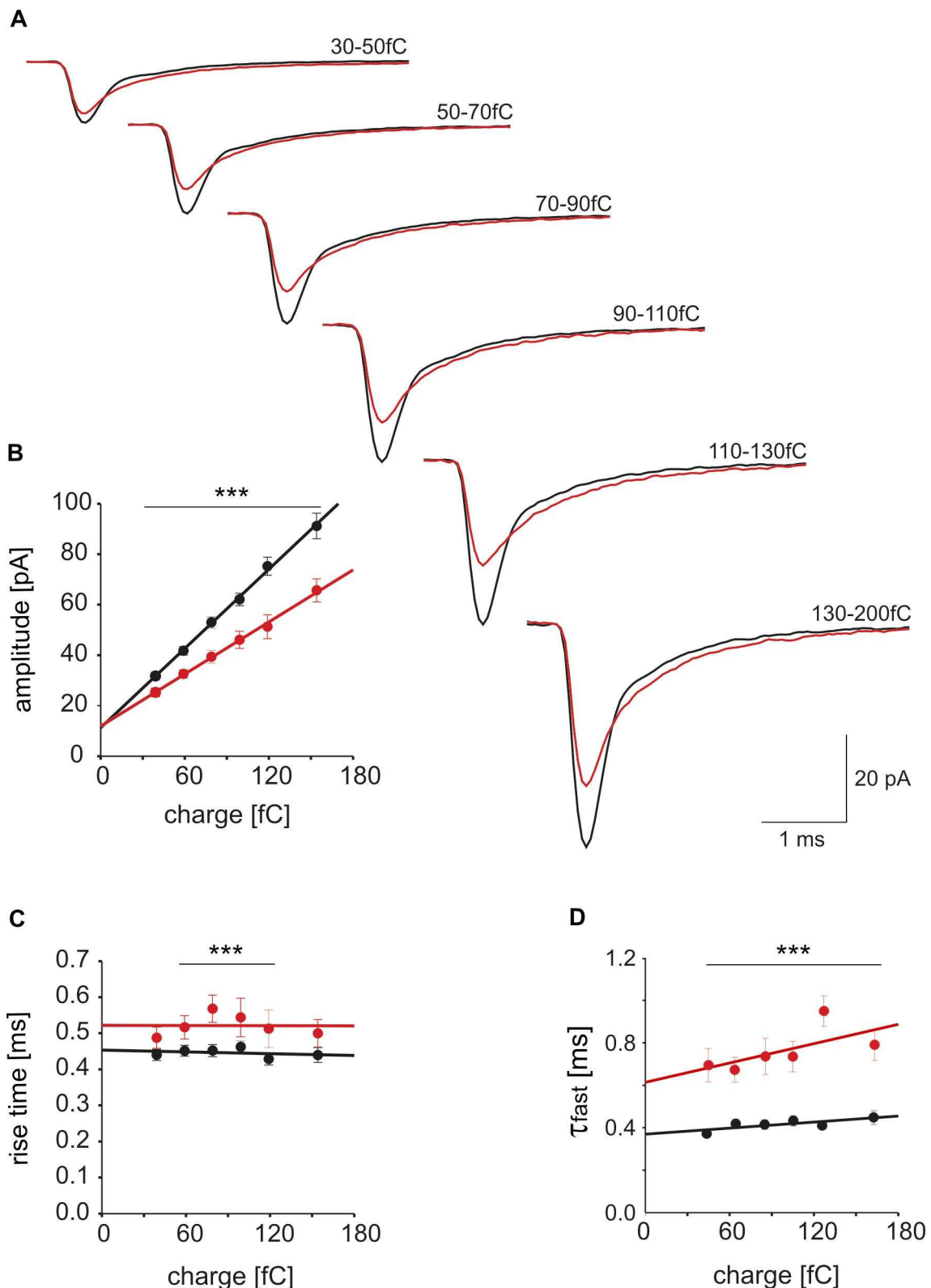


**Figure 16. Alterations in the time course of mutant signals are independent of quantal charge.** A) Averaged mEPSCs with similar charge taken from SybII ko neurons expressing SybII wild type protein (black) or 11aa insertion (red). B) Slops of the correlation amplitude vs charge (pA vs fC) for SybII (Black) and 11aa insertion (red). The event's amplitude scales proportionally to the event's charge and is significantly reduced over the entire range of charges for 11aa signals. C and D) kinetic parameters like 10-90% rise time and  $\tau_{decay}$  are shifted to longer times for the mutant protein when compared with SybII-signals. (SybII: n=23, 11aa: n=16 cells, \*\*\*p<0.001, one-way analysis of variance).

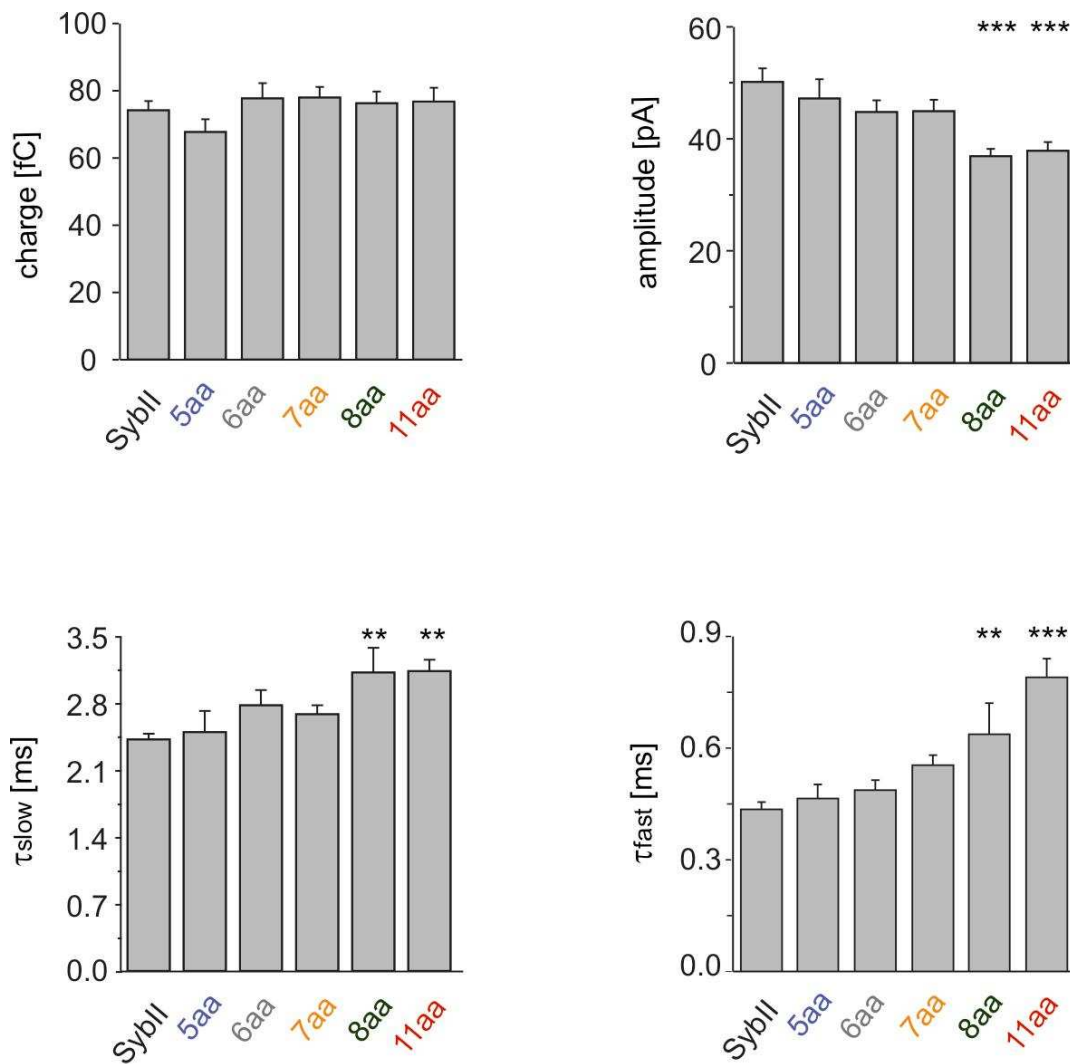


**Figure 17. Neurotransmitter release from small synaptic vesicles changes in a linker-length dependent fashion.** Extension of the juxtamembrane region (5aa, 6aa, 7aa, 8aa, and 11aa) significantly reduces mEPSC amplitude in longer linkers insertion and progressively prolongs neurotransmitter discharge without affecting the quantal size. Values are given as mean; SyblI (34), 5aa (13), 6aa (13), 7aa (22), 8aa (31), 11aa (21). \*\* $p < 0.01$ , \*\*\* $p < 0.001$ , one-way analysis of variance versus SyblI.

#### 4.8 SyblI action governs the time course of cleft glutamate

Motivated by the observations above, we studied whether the altered mEPSC time course could arise from a change in the temporal profile of glutamate experienced by the AMPA receptors as a result of a change in the kinetic of glutamate released from synaptic vesicles. To assess the extent of glutamate release during synaptic transmission, we made use of a previously established pharmacological approach (Liu et al., 1999). The rapidly dissociating competitive antagonist  $\gamma$ -D-glutamylglycine ( $\gamma$ -DGG), which competes with glutamate on the time-scale of AMPA-mEPSCs, partially attenuates glutamatergic release events in hippocampal synapses (Liu et al.,

1999). Because of the competitive nature of its interaction with glutamate, the degree of its attenuation is inversely related to the amount of glutamate being released, such that it can be used as a direct indicator of the speed of glutamate release. We used  $\gamma$ -DGG (200  $\mu$ M) to probe v-SNARE-dependent alterations in the peak glutamate concentration. If the cleft concentration of glutamate were significantly higher for SybII- than for 11aa-mediated events, one would expect that SybII and 11aa mEPSCs are less affected when challenged with a rapidly equilibrating blocker. To minimize the loss of events below the amplitude threshold (15 pA), we restricted our analysis to recordings with an average minimum event charge of 100 fC. Application of  $\gamma$ -DGG results in a reversible reduction of the mEPSC peak amplitude (Figure 18A,B).

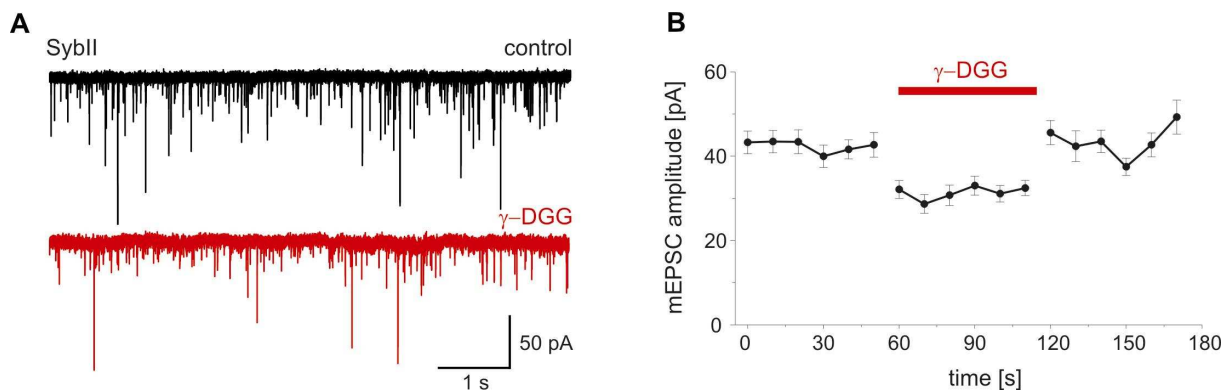


**Figure 18.  $\gamma$ -DGG effect causes a reversible attenuation of the mEPSC amplitude.** A) Exemplary traces of spontaneous mEPSC mediated by SybII in the absence (black trace; control) and in the presence of 200  $\mu$ M  $\gamma$ -DGG (red trace). B) Application of  $\gamma$ -DGG (red bar) is bracketed by control runs with superfusion of ringer's solution.

A comparison of averaged mEPSCs from before and after antagonist application at neurons expressing either SybII (left traces) or 11aa mutant proteins (right traces) depicts sample peak amplitude attenuation of SybII and 11aa (Figure 19A). As shown, application of  $\gamma$ -DGG results in a relative reduction of the mEPSC peak amplitude that is significantly stronger for 11aa events than for SybII events. Visualizing the amplitude distribution of the events confirms that  $\gamma$ -DGG causes pronounced leftward shift of the 11aa distribution relative to SybII (Figure 19B). On the whole,  $\gamma$ -DGG reduced the amplitude of the SybII mediated events by  $15.0 \pm 2.2$  % in contrast to  $25.3 \pm 5.2$  % by the 11aa insertion, (Figure 20A). On average, the efficacy of  $\gamma$ -DGG in attenuating the mEPSC peak amplitude is  $\sim 1.7$  fold stronger for the mutant than for the wt protein (Figure 20A). This line of experiments provided

evidence that the reduced mEPSC amplitude that we observed in signals mediated by mutant proteins is indeed a result of an altered kinetic of presynaptic glutamate release from SSV. The strong reduction in the frequency of the mutant signals caused by the antagonist (due to the loss of events below the detection threshold) is consistent with their lower amplitude (Figure 20B).

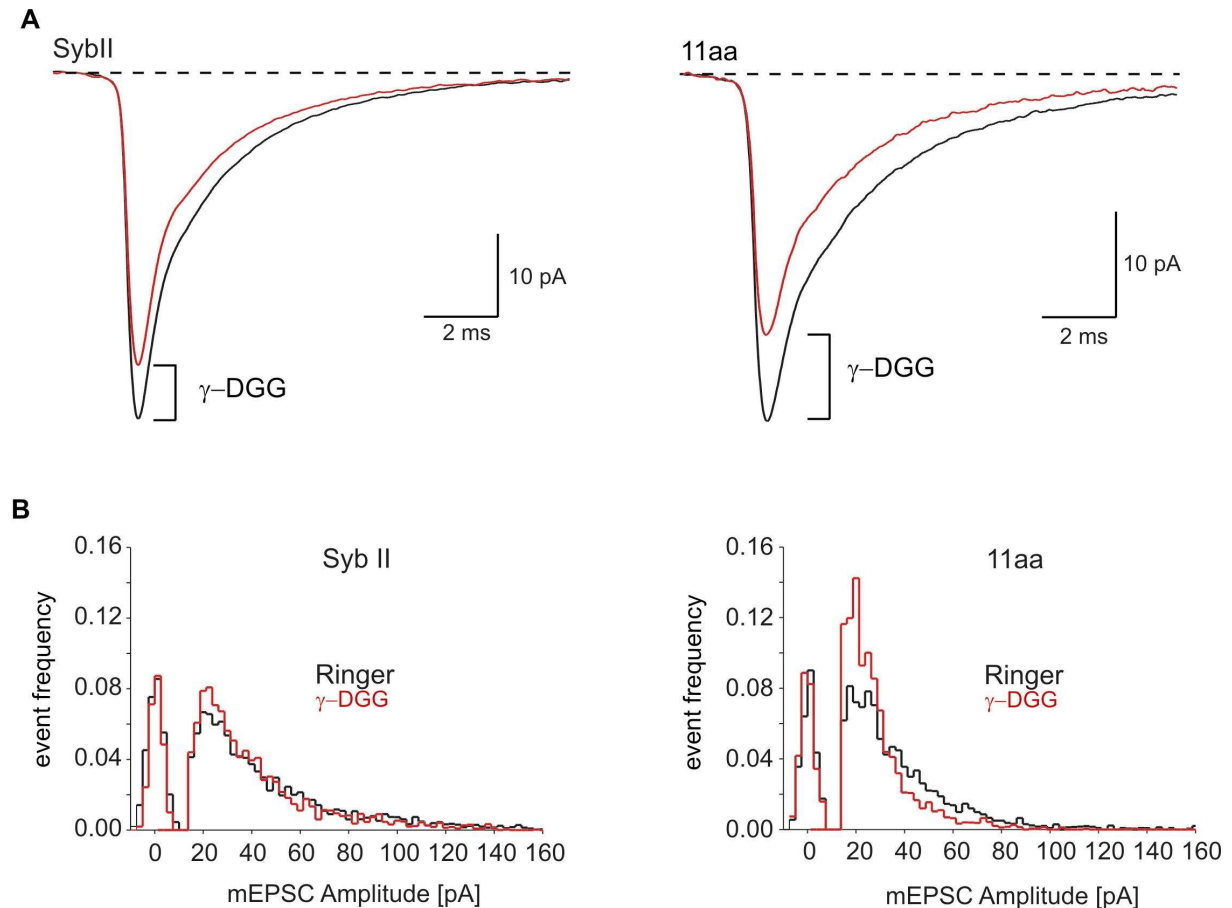


**Figure 19. Linker mutant produces a lower effective glutamate concentration than SybII.** A) Ensemble average of mEPSCs of cells expressing SybII (left, n=17) or the 11aa mutant (right, n=16) recorded in the absence (black trace) and in the presence of  $\gamma$ -DGG (red trace). Note the different scaling for the left and right panel. The relative inhibition is stronger for 11aa mutant (control: 109 fC, 33 pA,  $\gamma$ -DGG: 75 fC, 25 pA) than for SybII (control: 102 fC, 42 pA,  $\gamma$ -DGG: 82 fC, 35 pA). B) Peak amplitude distributions of the mEPSCs in the absence (black) and during exposure of  $\gamma$ -DGG (red) for SybII (left) and the 11aa insertion (right). Background noise distributions (peak centred at 0 pA) were obtained from 10-20 ms of recordings in which no mEPSCs were evident.

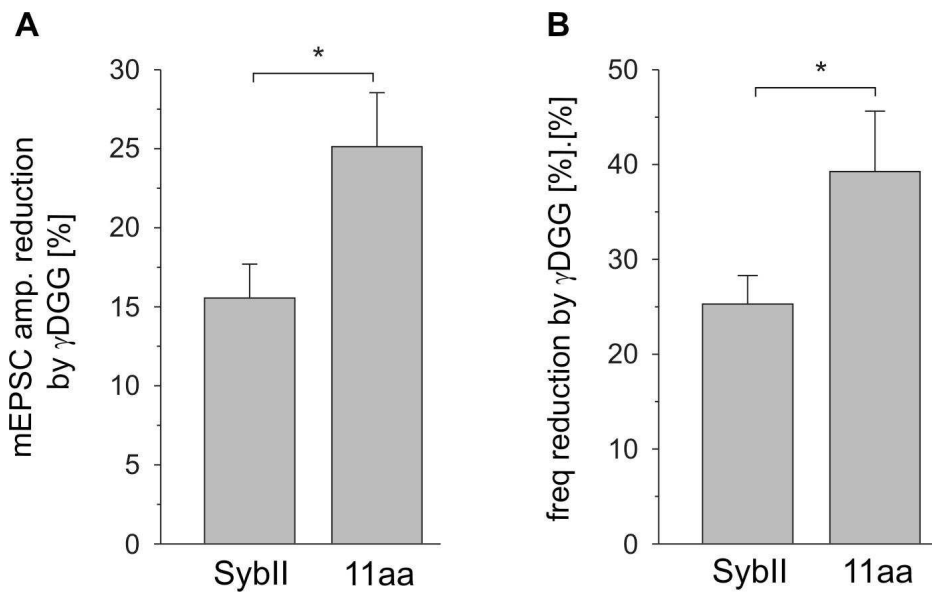


**Figure 20. Effect of  $\gamma$ -DGG on mEPSC amplitude and frequency.** A) mEPSC amplitude reduction by  $\gamma$ -DGG and B) frequency reduction by  $\gamma$ -DGG. 11aa events are more sensitive to  $\gamma$ -DGG than that of SybII events (SybII,  $n = 17$ ; 11aa,  $n = 16$ ,  $*p < 0.05$ , one-way analysis of variance).

Interestingly, the first component of the SybII mEPSC is less attenuated by the antagonist than its second component (Figure 21A), suggesting that these kinetically distinct phases are governed by different transmitter concentrations. In contrast, a nearly uniform degree of  $\gamma$ -DGG inhibition is observed for the first and the second phase of the mutant signal. The latter result confirms the view that the mutant protein slows transmitter discharge from SSVs, producing lower peak transmitter concentrations during the initial phase of the mEPSC signal. The time course of decay of the first and the second phase is only moderately but not significantly accelerated by  $\gamma$ -DGG (Figure 21B). This is possible, because the expected acceleration of the mEPSC time course might in part be compensated by reduced desensitization of the postsynaptic receptors in the presence of the competitive antagonist (Wong et al., 2003). Taken together, the experiments indicate that mutant-mediated exocytosis produces lower effective glutamate concentrations than the wild type protein. They suggest that v-SNARE force governs the time course of transmitter release from SSVs and thereby controls the temporal profile of cleft glutamate and the quantal signal.

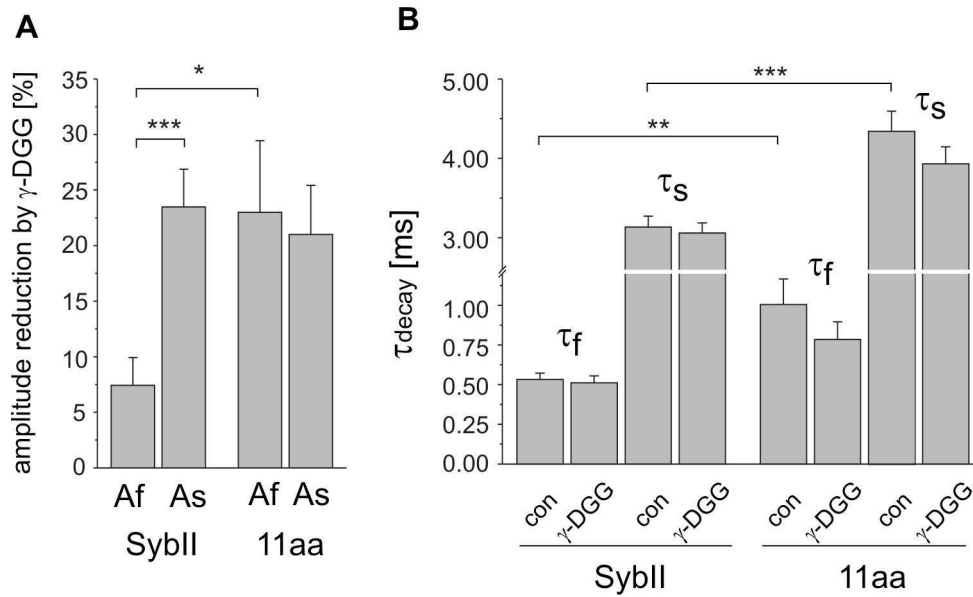


**Figure 21.  $\gamma$ -DGG effect on the two distinct components of release.** A) Differential effect of  $\gamma$ -DGG on the magnitude of the fast (Af) and slow (As) component of the mEPSC decays measured for SybII and 11aa signals. C) Mean mEPSC  $\tau_{decay}$  in the presence and in the absence of  $\gamma$ -DGG for both SybII and 11aa. The decay time constants,  $\tau_{fast}$  ( $\tau_f$ ) and  $\tau_{slow}$  ( $\tau_s$ ), are significantly slower for the mutants signals compared with SybII and are slightly faster in the presence of  $\gamma$ -DGG. (SybII, n= 17; 11aa, n= 16, \*p<0.05, \*\*p<0.01, \*\*\*p<0.001 one-way analysis of variance).

## **5 Discussion**

A fundamental question in synaptic physiology is to what extent the exocytotic release machinery influences synaptic efficacy. The goal of this study was to address the functional relevance of the SNARE machinery in particular the v-SNARE protein Synaptobrevin II in controlling the release readiness of SSV as well as the strength of quantal synaptic transmission. The results in this thesis show how key properties of the exocytosis mechanism gradually change by increasing the molecular distance between SNARE domain and TMD of Synaptobrevin II. They provide direct evidence for action of SNAREs in shaping the concentration profile of cleft glutamate and the quantal signal at fast glutamatergic synapses. Thus, SNARE proteins do not simply initiate SSV exocytosis, but also drive neurotransmitter release from SSVs and are crucial for the exquisite temporal regulation of neuronal signalling.

### **5.1 Linkers impair priming and stimulus secretion coupling of small synaptic vesicles**

The size of the readily releasable pool is a primary determinant of synaptic efficacy (Rosenmund and Stevens, 1996) and depends on SNARE proteins, as judged from the analysis of various SNARE null mutants (Schoch et al., 2001; Borisovska et al., 2005; Sørensen et al., 2003). The experiments demonstrate that extending the juxtamembrane region of SybII gradually reduces the action potential evoked response and delays the stimulus secretion coupling. Neither differences in the expression levels of the protein variants nor changes in the number of synapses were detected, rendering the possibility unlikely that the linker phenotype is caused by inefficient protein targeting or synapse formation. Instead, the results suggest that distance and/or flexibility between SNARE motif and the TMD controls the magnitude of the action potential evoked response. In close correlation, we observe a linker-length dependent reduction in the pool of primed vesicles, as judged by hypertonic sucrose application. The latter phenotype contrasts with observations for null mutants of Complexin or Synaptotagmin at hippocampal synapses, indicating that linker mutations do not interfere with binding of Complexin or Synaptotagmin to the SNARE complex (Geppert et al., 1994; Xue et al., 2008). Taken together, these results show that efficient priming of SSVs demands a tight molecular link between the SNARE

domain and the TMD of SybII. Priming of secretory vesicles is a complex process that involves a large variety of synaptic proteins (Südhof, 2004). In contrast, only a few molecular steps should be required to initiate fusion of SSVs at the millisecond time scale in response to the rapid release-site  $\text{Ca}^{2+}$ -transient. The experiments show that extending the juxtamembrane region of SybII systematically increases the time lag between the stimulus and the onset of exocytosis. Since linker mutations do not change the  $\text{Ca}^{2+}$ -sensitivity of secretion (Kesavan et al., 2007), it seems safe to conclude that a tight intramolecular coupling between the SNARE domain and the transmembrane anchor of SybII determines the millisecond time lag of SSV exocytosis. Thus, SNARE complex formation exerts mechanical force that is transmitted to membranes and initiates fusion of SSVs at the moment of the  $\text{Ca}^{2+}$ -rise. Given that SSVs experience only a transient  $\text{Ca}^{2+}$ -increase during an action potential, the altered release probability observed for the mutant proteins may be the consequence of delayed stimulus-secretion coupling. Taken together, both reductions in RRP and release probability contribute to the decreased synaptic response recorded for mutant proteins.

## **5.2 v-SNARE action drives rapid transmitter release from SSV**

Quantal release of neurotransmitter is the elementary signal of neuronal communication. In excitatory glutamatergic synapses, remarkable progress has been made in detailing the postsynaptic factors that regulate synaptic efficacy (Malenka and Nicoll, 1999), but comparatively less has been done to identify corresponding presynaptic mechanisms that influence the activation of postsynaptic receptors. In fact, to what extent the exocytotic machinery governs transmitter discharge from SSVs at CNS synapses and how it controls properties of quantal signalling is unknown.

Our experiments show that flexible insertions into the juxtamembrane region of SybII attenuate the amplitude and slow the decay of the mEPSC in a linker-length dependent fashion. These results suggest that SNARE protein-generated membrane stress provides an essential force not only to initiate fusion but also to hasten membrane merger. Given that SNAREs like SNAP-25 have been implicated in the trafficking of glutamate receptors (Lan et al., 2001; Washbourne et al., 2004), one

might speculate that the observed effects are due to changes in the number, spatial organisation or subunit composition of postsynaptic receptors at the release site. Several lines of evidences render these possibilities unlikely. First, detailed analyses reveal that linker mutations selectively change the amplitude and the time course of the quantal signal without altering its charge, which counters the possibility that mutant-mediated events engage a lower number of postsynaptic receptors than SybII events. Secondly, misalignment of postsynaptic receptors relative to the site of release should cause a reduction in amplitude together with an increase in the event's rise time, but cannot account for the strong changes in the decay time course Figure 16. Furthermore, 'off-center' release should be again accompanied with a profound decrease in charge transfer per SSV signal (Franks et al., 2003; Wu et al., 2007), which is not evident from the data. Third, potential alterations in the properties of the postsynaptic receptors are unlikely to be responsible for the mutant phenotype, because the subunit composition of glutamate receptors does not change in hippocampal synapses that were chronically treated with tetanus toxin to specifically inactivate SybII (Harms et al., 2005). Fourth, the mutant-mediated effects on SSV signals are in excellent agreement with our previous findings, showing that extending SybII's juxtamembrane region slows transmitter discharge from chromaffin granules (Kesavan et al., 2007). Taken together, the results indicate a presynaptic origin of the mutant phenotype. Given that SSVs release their content on a time scale of ~ 200 microseconds as judged from amperometric measurements (Bruns and Jahn, 1995; Bruns, 2004), the difference in time constant of decay ( $\tau_{fast}$ , Figure 13B) between wild type and mutant mEPSCs suggests a 2 to 3fold slowing of transmitter release by extending the juxtamembrane region of SybII. Taken together, v-SNARE action provides an essential force for rapid transmitter release from SSVs determining amplitude and kinetic properties of fast quantal glutamatergic transmission.

Consistent with these findings, we observe that the low affinity receptor antagonist  $\gamma$ -DGG attenuates mutant events more strongly than SybII events. These experiments reinforce the hypothesis that mutant exocytosis produces lower effective glutamate concentrations in the synaptic cleft than SybII exocytosis. Most likely, SNARE force governs fusion pore characteristics and thereby changes the transmitter concentration profile in the synaptic cleft and the resulting unitary postsynaptic current. Interestingly, the fast and the slow component of the SybII mEPSC decay

are diminished by  $\gamma$ -DGG to a different degree. Theoretical simulations of the mEPSC time-course suggested that receptor deactivation in response to the initial decline of the transmitter concentration governs the decay of the fast component, whereas persistence of a low concentration of glutamate in the synaptic cleft contributes to the subsequent slow component of the mEPSC (Silver et al., 1996; Diamond and Jahr, 1997; Wahl et al., 1996). The differential sensitivity of the fast and slow phase to  $\gamma$ -DGG is compatible with such a scenario, indicating that receptors mediating the slow tail of the mEPSC are activated by lower glutamate concentrations than during the mEPSC peak phase. In the same line, the stronger inhibition of the initial component of the mutant mEPSC suggests a lower rate of glutamate efflux from small synaptic vesicles than for SybII. Taken together, these observations predict a biphasic concentration waveform of cleft glutamate, which underlies the SSV event, where the first phase is determined in magnitude and kinetics by the rate of v-SNARE mediated transmitter release and the second phase is dominated by slow clearance of transmitter from the synaptic cleft. We would like to emphasize that these results do not exclude the possibility that desensitization of AMPA receptors contributes to the mEPSC decay (Trussell et al., 1989; Jones and Westbrook, 1996).

Previous studies have suggested, that modulation of quantal size is associated with alterations in the mode of exocytosis changing between either full collapse of the vesicle into the plasma membrane or its rapid retrieval (kiss and run mode, Harata et al., 2006). The observation that v-SNARE-generated membrane stress alters the unitary postsynaptic current, most likely by regulating fusion pore expansion, identifies this mechanism as an attractive target for switching fusion modes of SSVs. Considering this result in the context of trans-SNARE complexes, one might expect that weakening the mechanical coupling between the SNARE domain and the TMD for both v- and t-SNARE proteins should cause an even further reduction of the mEPSC amplitude.

Heterogeneity in the speed of glutamate release from single vesicles has been implicated for a number of important mechanisms that are central to development and plasticity of the central nervous system (Choi et al., 2003; Zakharenko et al., 2002; Chen et al., 2004). Likewise, perturbing synaptic vesicle fusion with tetanus toxin, reverts functional to silent transmission and slows NMDA activation (Renger et

al., 2001), which is consistent with our observation that SNARE-mediated membrane stress is a determinant factor for the rate of transmitter release from single vesicles. *In vitro* studies indicated that the energy of several SNARE complexes is required to make a vesicle fuse (Li et al., 2009; Domanska et al., 2009). Thus, SNARE mediated membrane fusion should be determined by the efficacy of force transfer between the SNARE domain and the transmembrane anchor and the number of productive SNARE complexes engaged per fusion event. Intriguingly, the time course of quantal signals changes during development of brain synapses in a remarkably similar fashion as observed for events mediated by SybII and the mutant proteins (Yamashita et al., 2003; Cathala et al., 2005), pointing to the possibility that alterations in SNARE force contribute to the speeding of mEPSC at mature brain synapses. Taken together, my experiments elucidate a new avenue to control neuronal communication, wherein changing SNARE force determines synaptic strength not only by controlling the release readiness of SSVs at CNS synapses but also by regulating the speed of glutamate release from the single synaptic vesicle.

## 6 Bibliography

Barbour B., Keller, U., Llano I., and Marty A. (1994). Prolonged presence of glutamate during excitatory synaptic transmission to cerebellar Purkinje cells. *Neuron*. 12, 1331–1343.

Barrett F, Stevens F. (1972). The kinetics of transmitter release at the frog neuromuscular junction. *J. Physiol.* 227, 691–708.

Baumert M., Maycox P. R., Navone F., De Camilli P. and Jahn R. (1989). Synaptobrevin: an integral membrane protein of 18,000 daltons present in small synaptic vesicles of rat brain. *EMBO J.* 8, 379–384.

Bennett M. K., Calakos N. and Scheller R. H. (1992). Syntaxin: a synaptic protein implicated in docking of synaptic vesicles at presynaptic active zones. *Science* 257, 255–259.

Bekkers J. Richerson G. and Stevens C. (1990). Origin of variability in quantal size in cultured hippocampal neurons and hippocampal slices. *Proc. Natl. Acad. Sci. USA.* 87, 5359-5362

Bekkers, J., and Stevens, C. (1991). Excitatory and inhibitory autaptic current in isolated hippocampal neurons maintained in cell culture. *Proc. Natl. Acad. Sci. USA* 88, 7834-7838.

Borisovska, M., Zhao Y., Tsytsyura Y., Glyvuk N., Takamori S., Matti U., Rettig J., Südhof T., Bruns D. (2005). v-SNAREs control exocytosis of vesicles from priming to fusion. *EMBO J.* 24, 2114-26.

Broadie K., Prokop A., Bellen H. J., O’Kane C. J., Schulze K. L. and Sweeney S. T. (1995), Syntaxin and synaptobrevin function downstream of vesicle docking in *Drosophila*. *Neuron*. 15, 663–673.

Bruns, D., and Jahn, R. (1995). Real-time measurement of transmitter release from single synaptic vesicles. *Nature* 377, 62-65.

Bruns D. (1998). Serotonin transport in cultured leech neurons. *Methods Enzymol.* 296, 593-607.

Bruns D. and Jahn R. (2002), Molecular determinants of exocytosis. *Pflugers Arch.* 443, 333–338.

Bruns, D. (2004). Detection of transmitter release with carbon fiber electrodes. *Methods Enzymol.* 33, 312-21.

Bouron Alexandre. (2001). Modulation of spontaneous quantal release of Neurotransmitters in the hippocampus. *Prog neurobiol.* 63, 613-635.

Carr C. and Munson M., (2007), Tag team action at the synapse. *EMBO rep.* 9, 834-8.

Cathala L., Holderith N., Nusser Z., Digregorio D. and Cull-Candy S. (2005). Changes in synaptic structure underlie the developmental speeding of AMPA receptor-mediated EPSCs. *Nat. Neurosci.* 10, 1310-1318.

Calhoun C. and Goldenring R. (1997). Two Rab proteins, vesicle-associated membrane protein 2 (VAMP-2) and secretory carrier membrane proteins (SCAMPs), are present on immunisolated parietal cell tubulovesicles. *Biochem. J.* 325, 559–564.

Chapman R. and Jahn R. (1994) Calcium-dependent interaction of the cytoplasmic region of synaptotagmin with membranes. Autonomous function of a single C2-homologous domain. *J. Biol. Chem.* 269, 5735–574.

Chen L., Chetkovich D., Petralia R., Sweeney N., Kawasaki Y., Wenthold R., Brecht D., Nicoll R. (2000). Stargazin regulates synaptic targeting of AMPA receptors by two distinct mechanisms. *Nature.* 408, 936–943.

Chen G. Harata N. and Tsien R. (2004). Paired-pulse depression of unitary quantal amplitude at single hippocampal synapses. *PNAS*. 101, 1063-1068.

Choi S. Klingauf F. and Tsien R. (2000). Postfusional regulation of cleft glutamate concentration during LTP at 'silent synapses'. *Nature Neurosci.* 3, 330-336.

Choi S., Klingauf J., and Tsien R. (2003). Fusion pore modulation as a presynaptic mechanism contributing to expression of long-term potentiation. *Phil. Trans. R. Soc. Lond.* 358, 695-705.

Clements J., Lester R., Tong G., Jahr, C., and Westbrook G. (1992). The time course of glutamate in the synaptic cleft. *Science*, 258, 1498–1501.

Diamond J. and Jahr C. (1997). Transporters buffer synaptically released glutamate on a submillisecond time scale. *J. Neurosci.* 17, 4672-4687.

Dietrich D., Kirschstein T., Kukley M., Pereverzev A., von der Brelie, C., et al. (2003). Functional specialization of presynaptic Cav2.3 Ca<sup>2+</sup> channels. *Neuron* 39,483–96.

Dresbacha T., Qualmanna B., Kesselsa M., Garnerb C. And Gundelfingera E. (2001). The presynaptic cytomatrix of brain synapses. *Cell. Mol. Life Sci.* 58, 94–116.

Eric R., Kandel H., Schwartz and Tomas M. (1991). Jessell. Principles of neuronal science. ELSEVIER, Third edition, pp. 19-36.

Fasshauer D., Sutton R. B., Brunger A. T. and Jahn R. (1998). Conserved structural features of the synaptic fusion complex: SNARE proteins reclassified as Q- and R-SNAREs. *Proc. Natl. Acad. Sci. USA.* 95, 15781–15786.

Finley M., Patel S., Madison D. and Scheller R. (2002). The core membrane fusion complex governs the probability of synaptic vesicle fusion but not transmitter release kinetics. *J. Neurosci.* 22, 1266–1272.

Franks K., Stevens C., and Sejnowski. (2003). Independent sources of quantal variability at single glutamatergic synapses. *J. Neurosci.* 23, 3186-3195.

Freneau, R., Kam K., Qureshi T., Johnson J., Copenhagen D., Storm-Mathisen J., Chaudhry F., Nicoll R., Edwards R. (2004). Vesicular glutamate transporters 1 and 2 target to functionally distinct synaptic release sites. *Science* 304, 1815-1819.

Fon E. and Edwards R. (2001). Molecular mechanisms of neurotransmitter release. *Muscle Nerve.* 5, 581-601.

Follenzi A., Sabatino G., Lombardo A., Boccaccio C. and Naldini L. (2002). Efficient gene delivery and targeted expression to hepatocytes in vivo by improved lentiviral vectors. *Hum. Gene Ther.* 13, 243-260.

Follenzi A., Ailles L., Bakovic S., Geuna M. and Naldini L. (2000). Gene transfer by lentiviral vectors is limited by nuclear translocation and rescued by HIV-1 pol sequences. *Nat. Genet.* 25, 217-222.

Forti L., Bossi M., Bergamaschi A., Villa A., and Malgaroli A. (1997). Loose-patch recordings of single quanta at individual hippocampal synapses. *Nature* 388, 874-878.

Gaisano H. Y., Sheu L., Foskett J. K. and Trimble W. S. (1994). Tetanus toxin light chain cleaves a vesicle-associated membrane protein (VAMP) isoform 2 in rat pancreatic zymogen granules and inhibits enzyme secretion. *J. Biol. Chem.* 269, 17062-17066.

Geppert M., Goda Y., Hammer R., Li C., Rosahl T., Stevens C., Südhof T. (1994). Synaptotagmin I: a major  $Ca^{2+}$  sensor for transmitter release at a central synapse. *Cell* 79, 717-27.

Grote E., Hao J. C., Bennett M. K. and Kelly R. B. (1995). A targeting signal in VAMP regulating transport to synaptic vesicles. *Cell* 81, 581-589.

Gerst J. (1997) Conserved alpha-helical segments on yeast homologs of the synaptobrevin/VAMP family of v-SNAREs mediate exocytic function. *J. Biol. Chem.* 272, 16591–16598.

Hagler D. and Goda Y. (2001). Properties of synchronous and asynchronous release during pulse train depression in cultured hippocampal neurons. *J. Neurophysiol.* 85, 2324–34.

Hao J., Salem N., Peng X., Kelly R. and Bennett M. (1997). Effect of mutations in vesicle-associated membrane protein (VAMP) on the assembly of multimeric protein complexes. *J. Neurosci.* 17, 1596–1603.

Harms K. Tovar K. and Craig A. (2005). Synapse-specific regulation of AMPA receptor subunit composition by activity. *J. Neurosci.* 25, 6379-6388.

Hashimoto K, Fukaya M, Qiao X, Sakimura K, Watanabe M, Kano M (1999). Impairment of AMPA receptor function in cerebellar granule cells of ataxic mutant mouse stargazer. *J Neurosci.* 19, 6027–6036.

Hayashi T., McMahon H., Yamasaki S., Binz T., Hata Y., Sudhof T. C. et al. (1994). Synaptic vesicle membrane fusion complex: action of clostridial neurotoxins on assembly. *EMBO J.* 13, 5051–5061.

Hestrin S., Sah P. and Nicoll R. (1990). Mechanisms generating the time course of dual component excitatory synaptic currents recorded in hippocampal slices. *Neuron*, 5, 247–253.

Hestrin S. (1992). Activation and desensitization of glutamate-activated channels mediating fast excitatory synaptic currents in the visual cortex. *Neuron*, 9, 991–999.

Hollmann M. And Heinemann S. (1994). Cloned glutamate receptors. *Annu Rev Neurosci.* 17, 31-108.

Inoue A., Obata K. and Akagawa K. (1992). Cloning and sequence analysis of cDNA for a neuronal cell membrane antigen, HPC-1. *J. Biol. Chem.* 267, 10613–10619.

Ishikawa T., Sahara Y. and Takahashi T. (2002). A single packet of transmitter does not saturate postsynaptic glutamate receptors. *Neuron* 34, 613- 621.

Jahn R. and Sudhof T. C. (1999), Membrane fusion and exocytosis. *Annu. Rev. Biochem.* 68, 863–911.

Jahn R, Scheller R., (2006). SNAREs--engines for membrane fusion. *Nat Rev Mol Cell Biol.* 7, 631-643.

Jonas P., and Spruston N. (1994). Mechanisms shaping glutamate-mediated excitatory postsynaptic currents in the CNS. *Current Opinion in Neurobiology*,4, 366–372.

Jones M., and Westbrook G. (1996). The impact of receptor desensitization on fast synaptic transmission. *Trends neurosci.* 19, 96-101.

Kaech S. and Banker G. (2006). Culturing hippocampal neurons. *Nat. Protocols.* 1, 2406-2415.

Katz B. and Miledi R. (1969) Spontaneous and evoked activity of motor nerve endings in calcium Ringer. *J Physiol.* 3, 689-706.

Kesavan J., Borisovska M. and bruns D., (2007). V-SNARE actions during Ca<sup>2+</sup>-triggered exocytosis. *Cell.* 131, 351-363.

Kessels H. and Malinow R. (2009). Synaptic AMPA Receptor Plasticity and Behavior. *Neuron.* 61, 340-350.

Kupra B. and Liu G. (2004). Does the fusion pore contribute to synaptic plasticity? *Trends Neurosci.* 27, 62-66.

Lan J., Skeberdis V., Jover T., Grooms S., Lin Y., Araneda R., Zheng X., Bennett M., Zukin R. (2001). Protein kinase C modulates NMDA receptor trafficking and gating. *Nat. Neurosci.* 4, 382-390.

Li F., Pincet F., Perez E., Eng W., Melia T., Rothman J., Tareste D. (2009). Energetics and dynamics of SNAREpin folding across lipid bilayers. *Nat. Struct. Mol. Biol.* 14, 890-896.

Livsey C., Costa E., and Vicini S. (1993). Glutamate-activated currents in outside-out patches from spiny versus aspiny hilar neurons of rat hippocampal slices. *Journal of Neuroscience*, 13, 5324–5333.

Liu S-Q. and Cull-Candy S (2000). Synaptic activity at calcium-permeable AMPA receptors induces a switch in receptor subtype. *Nature*. 405, 454–458.

Lüscher C, Nicoll R, Malenka R, Muller D (2000). Synaptic plasticity and dynamic modulation of the postsynaptic membrane. *Nat Neurosci.* 3, 545–550.

Liu G., Choi S. and Tsien R. (1999). Variability of neurotransmitter concentration and nonsaturation of postsynaptic AMPA receptors at synapses in hippocampal cultures and slices. *Neuron*. 22, 395-409.

Liu G., Tsien RW. (1995). Properties of synaptic transmission at single hippocampal synaptic boutons. *Nature*. 375, 404–408.

Lin RC and Scheller RH. (2000), Mechanisms of synaptic vesicle exocytosis. *Annu Rev Cell Dev Biol.* 16, 19–49.

Lisman J., Raghavachari S. and Tsien R. (2007). The sequence of events that underlie quantal transmission at central glutamatergic synapses. *Nature Reviews Neuroscience*. 8, 597-609.

Littleton J., Chapman E., Kreber R., Garment M., Carlson S. and Ganetzky B. (1998). Temperature-sensitive paralytic mutations demonstrate that synaptic exocytosis requires SNARE complex assembly and disassembly. *Neuron* 21, 401–413.

Magleby K., and Stevens C. (1972). A quantitative description of end-plate currents. *Journal of Physiology London*, 223, 173–197.

Malinow R., and Malenka R (2002). AMPA receptor trafficking and synaptic plasticity. *Annu Rev Neurosci.* 25,103–126.

Malenka R., and Nicoll R (1999). Long-term potentiation: a decade of progress? *Science* 285, 1870–1874.

Man HY, Ju W., Ahmadian G., Wang Y. (2000). Intracellular trafficking of AMPA receptors in synaptic plasticity. *Cell Mol Life Sci.* 57, 1526–1534.

Mayer A. (2001). What drives membrane fusion in eukaryotes? *Trends Biochem. Sci.* 26, 717–723.

Mennerick S., and Zorumski C. (1995). Presynaptic influence on the time course of fast excitatory synaptic currents in cultured hippocampal cells. *J. Neurosci.* 15, 3178-3192.

Misonou H., Ohara-Imaizumi M. and Kumakura K. (1997). Regulation of the priming of exocytosis and the dissociation of SNAP-25 and VAMP-2 in adrenal chromaffin cells. *Neurosci. Lett.* 232, 182–184.

Montecucco C. and Schiavo G. (1993). Tetanus and botulism neurotoxins: a new group of zinc proteases. *Trends Biochem. Sci.* 18: 324–327.

Nakanishi S., and Masu M. (1994). Molecular diversity and functions of glutamate receptors. *Annu Rev Biophys Biomol Struct.* 23, 319-48.

Nielsen S., Marples D., Birn H., Mohtashami M., Dalby N. O., Trimble M. et al. (1995) Expression of VAMP-2-like protein in kidney collecting duct intracellular vesicles. Colocalization with Aquaporin-2 water channels. *J. Clin. Invest.* 96, 1834–1844.

Nickel W., Weber T., McNew J., Parlati F., Söllner T., Rothman J. (1999). Content mixing and membrane integrity during membrane fusion driven by pairing of isolated v-SNAREs and t-SNAREs. *Proc. Natl. Acad. Sci. USA* 96, 12571-12576.

O'Connor V., Heuss C., De Bello W. M., Dresbach T., Charlton M. P., Hunt J. H. et al. (1997). Disruption of syntaxin-mediated protein interactions blocks neurotransmitter secretion. *Proc. Natl. Acad. Sci. USA* 94, 12186–12191.

Olson A., Knight J. and Pessin J. (1997). Syntaxin 4, VAMP2 and/or VAMP3/cellubrevin are functional target membrane and vesicle SNAP receptors for insulin-stimulated GLUT4 translocation in adipocytes. *Mol. Cell. Biol.* 17, 2425–2435.

Oyler G., Higgins G., Hart R., Battenberg E., Billingsley M., Bloom F. et al. (1989). The identification of a novel synaptosomal-associated protein, SNAP-25, differentially expressed by neuronal subpopulations. *J. Cell Biol.* 109, 3039–3052.

Pobbati A., Stein A., and Fasshauer D. (2006). N- to C-terminal SNARE complex assembly promotes rapid membrane fusion. *Science* 313, 673-676.

Reim K, Mansour M, Varoqueaux F, McMahon HT, Sudhof TC, Brose N, Rosenmund C (2001). Complexins regulate a late step in Ca<sup>2+</sup>-dependent neurotransmitter release. *Cell.* 104, 71–81.

Regazzi R., Wollheim C. B., Lang J., Theler J. M., Rossetto O., Montecucco C. et al. (1995). VAMP-2 and cellubrevin are expressed in pancreatic beta-cells and are essential for Ca<sup>2+</sup> but not for GTP gamma S-induced insulin secretion. *EMBO J.* 14, 2723–2730.

Regazzi R., Sadoul K., Meda P., Kelly R. B., Halban P. A. and Wollheim C. B. (1996). Mutational analysis of VAMP domains implicated in Ca<sup>2+</sup>-induced insulin exocytosis. *EMBO J.* 15, 6951–6959.

Renger J., Egles C. and Liu G. (2001). A developmental switch in neurotransmitter flux enhances synaptic efficacy by affecting AMPA receptor activation. *Neuron* 29, 469-484.

Rizo J. and Sudhof T. C. (2002), Snares and munc18 in synaptic vesicle fusion. *Nat. Rev. Neurosci.* 3, 641–653.

Rizzoli S., and Betz W. (2005). Synaptic vesicle pools. *Nat. Rev. Neurosci.* 6, 57-69

Rosenmund, C., Rettig, J. and Brose, N., (2003). Molecular mechanisms of active zone function. *Curr Opin Neurobiol.* 5, 509-19.

Rosenmund C., Sternbach Y. and Stevens C. (1998). The tetrameric structure of a glutamate-receptor channel. *Science.* 280, 1596–1599.

Rosenmund C. and Stevens C. (1996). Definition of readily releasable pool of vesicles at hippocampal synapses. *Neuron.* 16, 1197-1207.

Rothman J. E. (1994). Mechanisms of intracellular protein transport. *Nature.* 372, 55–63.

Sabatini B., Regehr W. (1996). Timing of neurotransmission at fast synapses in the mammalian brain. *Nature.* 384, 170–72.

Schuetz C., Hatsuzawa K., Margittai M., Stein A., Riedel D., Küster P., König M., Seidel C. and Jahn R. (2004). Determinants of liposome fusion mediated by synaptic SNARE proteins. *Proc. Natl. Acad. Sci. USA* 101, 2858-2863.

Tang C.-M., Shi Q.-Y., Katchman A. and Lynch G. (1991). Modulation of the time course of fast EPSCs and glutamate channel kinetics by aniracetam. *Science.* 254, 288–290.

Silver R., Colquhoun D. and Cull-Candy S. (1996) Edmonds B. Deactivation and desensitization of non-NMDA receptors in patches and time course of EPSCs in rat cerebellar granule cells. *J. Physiol.* 493.1, 167-173.

Sollner T., Whiteheart S. W., Brunner M., Erdjument-Bromage H., Geromanos S., Tempst P. et al. (1993). SNAP receptors implicated in vesicle targeting and fusion. *Nature* 362, 318–324.

Sørensen J., Nagy G., Varoqueaux F., Nehring R., Brose N., Wilson M., Neher E. (2003). Differential control of the releasable vesicle pools by SNAP-25 splice variants and SNAP-23. *Cell* 114, 75-86.

Südhof C. (2004). The synaptic vesicle cycle. *Annu. Rev. Neurosci.* 27, 509-47.

Sutton R., Fasshauer D., Jahn R. and Brunger A. (1998), Crystal structure of a SNARE complex involved in synaptic exocytosis at 2.4 Å resolution. *Nature* 395, 347–353.

Schiavo G., Benfenati F., Poulain B., Rossetto O., Polverino de Laureto P., DasGupta B. R. et al. (1992). Tetanus and botulinum-B neurotoxins block neurotransmitter release by proteolytic cleavage of synaptobrevin. *Nature.* 359, 832–835.

Schoch S., Deak F., Königstorfer A., Mozhayeva M., Sara Y., Südhof T. C. et al. (2001). SNARE function analyzed in synaptobrevin/VAMP knockout mice. *Science* 294: 1117– 1122

Trimble W. S., Cowan D. M. and Scheller R. H. (1988). VAMP-1: a synaptic vesicle-associated integral membrane protein. *Proc. Natl. Acad. Sci. USA* 85, 4538–4542.

Trussell L., Thio, L., Zorumski C., and Fischbach, G. (1988). Rapid desensitization of glutamate receptors in vertebrate central neurons. *Proceedings of the National Academy of Science U.S.A.*, 85, 2834–2838.

Trussell L. and Fischbach G. (1989). Glutamate receptor desensitization and its role in synaptic transmission. *Neuron*. 3, 209–218.

Trussell L., Zhang S., and Raman, I. (1993). Desensitization of AMPA receptors upon multiquantal neurotransmitter release. *Neuron*. 10, 1185–1196.

Tong G., and Jahr C. E. (1994). Multivesicular release from excitatory synapses of cultured hippocampal neurons. *Neuron*. 12, 51–59

Wah L., Pouzat C., and Stratford K. (1996). Monte carlo simulation of fast excitatory synaptic transmission at a hippocampal synapse. *J. neurophysiol.* 75, 597-608

Washbourne P., Liu X., Jones E., and MacAllister A. (2004) Cycling of NMDA receptors during trafficking in neurons before synapse formation. *J. Neurosci.* 24, 8253-64.

Weber T., Zemelman B., McNew J., Westermann B., Gmachl M., Parlati F., Söllner T. and Rothman J. (1998). SNAREpins: minimal machinery for membrane fusion. *Cell* 92, 759-772.

Weimbs T., Low S., Chapin S., Mostov K., Bucher P. and Hofmann K. (1997). conserved domain is present in different families of vesicular fusion proteins: a new superfamily. *Proc. Natl. Acad. Sci. USA.* 94, 3046–3051.

Wickner W. and Haas A. (2000). Yeast homotypic vacuole fusion: a window on organelle trafficking mechanisms. *Annu. Rev. Biochem.* 69, 247–275.

Wilson N., Kang J., Hueske E., Leung T., Varoqui H., Murnick J., Erickson J. and Liu G. (2005). Presynaptic regulation of quantal size by the vesicular glutamate transporter VGLUT1. *J. Neurosci.* 26, 6221-6234.

Wojcik S., Rhee J., Herzog E., Sigler A., Jahn R., Takamori S., Brose N., and Rosenmund C. (2004). An essential role for vesicular glutamate transporter 1

(VGLUT1) in postnatal development and control of quantal size. *Proc. Natl. Acad. Sci. USA.* 101, 7158 -7163.

Wong A., Graham B., Billups B., and Forsythe I. (2003). Distinguishing between presynaptic and postsynaptic mechanisms of short-term depression during action potential trains. *J. Neurosci.* 23, 4868-4877.

Wu X., Xue L., Mohan R., Paradiso K., Gillis K. and Wu L. (2007). The origin of quantal size variation: vesicular glutamate concentration plays a significant role. *J. Neurosci.* 27, 3046-3056.

Xue M., Stradomska A., Chen H., Brose N., Zhang W., Rosenmund C. and Reim K. (2008). Complexins facilitate neurotransmitter release at excitatory and inhibitory synapses in mammalian central nervous system. *Proc. Natl. Acad. Sci. USA.* 105, 7875-7880.

Yamashita T., Ishikawa T. and Takahashi T. (2003). Developmental increase in vesicular glutamate content does not cause saturation of AMPA receptors at the calyx of held synapses. *J. Neurosci.* 23, 3633-3638.

Yoshida A., Oho C., Omori A., Kuwahara R., Ito T. and Takahashi M. (1992). HPC-1 is associated with synaptotagmin and omega-conotoxin receptor. *J. Biol. Chem.* 267, 24925–24928.

Zakharenko S., Zablow L., and Siegelbaum S. (2002). Altered presynaptic vesicle release and cycling during mGluR-dependent LTD. *Neuron.* 35, 1099-1110.

Zhou Q. Petersen CC. Nicoll R. (2000). Effects of reduced vesicular filling on synaptic transmission in rat hippocampal neurones. *J. Physiol. (Lond).* 525, 195-206.

## 7 Publications

**Guzmán R.E.**, Bolaños P., Delgado A., Rojas H., DiPolo R., Caputo C., Jaffe E.H.. Depolymerisation and rearrangement of actin filaments during exocytosis in rat peritoneal mast cells: involvement of ryanodine-sensitive calcium stores. *Pflugers Arch - Eur J Physiol* (2007) 454:131–141.

**Guzman R.E.**, Yvonne Schwarz and Dieter Bruns. Presynaptic control of quantal synaptic transmission. *Submitted to Nature Neuroscience*.

### **Congress and special conferences**

38<sup>th</sup> Annual Meeting of Neuroscience 2008. Washington DC. December 15<sup>th</sup> –19<sup>th</sup>. The intramolecular distance between SNARE motif and transmembrane domain of Synaptobrevin II is crucial to synchronize neurotransmitter release. **Raul E. Guzman**, Yvonne Schwarz and Dieter Bruns

19<sup>th</sup> Neuro-DoWo (Neurobiology PhD student workshop) Saarbrücken, April 10<sup>th</sup>-11<sup>th</sup> 2008. "The intramolecular distance between SNARE motif and transmembrane domain of Synaptobrevin II is crucial to synchronize neurotransmitter release." **Guzman R.E.**, Schwarz Y., Bruns D.

35<sup>th</sup> Annual Meeting of Neuroscience 2005. Washington DC. November 12<sup>th</sup> –16<sup>th</sup>. Involvement of intracellular Ca<sup>2+</sup> stores in the depolymerization of actin filaments during exocytosis in rat peritoneal mast cells. E.H. Jaffe, **R. Guzman**, A. Delgado, P. Bolanos, C Caputo.

54 annual Meeting, ASOVAC Valencia, November 14<sup>th</sup> –21<sup>th</sup> 2004 Rearrangement of F-actin by latrunculin A potentiate exocytosis from rat peritoneal mast cell. **R. Guzman**, P Bolanos, E.H. Jaffe.

III Integrated Cellular Biology Postgraduate Studies Conference. December 06-08, 2004. Re arrangement of F-actin by latrunculin A potentiate exocytosis from rat peritoneal mast cell. **R. Guzman**.

## **8 Acknowledgements**

I would like to thank my supervisor Prof. Dr. Dieter Bruns to gave me stupendous teaching and support through out my PhD. He dedicated a lot of time for discussing results; his passion and enthusiasm for science provided me always encourages to persist my goals. He taught me not only how to design and perform experiments, but also to address science in a systematic manner and in different angles.

I also would like to thank all members of my department. Especially, Marina Wirth and Katja Klingler for their excellent technical assistance and professional support. I am extremely grateful to Ivonne N. Schwartz for being an exceptional person and for her constant help and cooperation.

I would like to take this opportunity to thank my family and wife for their love and encouragement.

## 9 Curriculum Vitae

**Name:** Raul Guzman Castro (Chemical Pharmacist)  
**Address:** Ortsstrasse 24, Homburg, Germany  
**Telephone:** +4917662179690  
**Date of Birth:** 16/04/1978  
**Nationality:** Colombian

### Education

Feb 1995 – August 2002      Chemical Pharmacist, University of Cartagena, Colombia.

March 2003-August 2005      Master in science, mention Biochemistry, Venezuelan Institute of Scientific Research (IVIC), Venezuela.

September 2005 – Present      Ph.D.-thesis with Prof. Dr. Dieter Bruns, Dept. for Cellular Physiology University of Saarland Saarland University (campus Homburg), Germany

### Research Experiences

March 2003 – Feb 2004      **Professional training** with Dr. Erica Jaffe at Venezuelan Institute of scientific research (IVIC), Venezuela.

March 2004-August 2005      **Electrophysiology MgSc** with Dr. Erica Jaffe at Venezuelan Institute of scientific research (IVIC), Venezuela.

September 2005 – Present      **Electrophysiology PhD Position** with Prof. Dr. Dieter Bruns at Saarland University (campus Homburg), Germany.

## **Awards Received**

University of Cartagena meritorious mention to licentiate thesis, 2002.

Venezuelan Institute of Scientific Research (IVIC) "Contingencia" scholarship holder (2003-2005)